Diplomarbeit

Shape Processing in the Human Brain

Wissenschaftliche Arbeit

zur Erlangung des Grades eines Diplom-Psychologen

im Fachbereich Psychologie

der Mathematisch-Naturwissenschaftlichen Sektion

der Universität Konstanz

vorgelegt von

Christian Friedrich Altmann

Erstgutachter : Professor Dr. Thomas Elbert

Zweitgutachter : Professor Dr. Heinrich H. Bülthoff

(Max-Planck-Institut für biologische Kybernetik, Tübingen)

Konstanz, Dezember 2001

Acknowledgements:

I would like to thank Dr. Zoe Kourtzi for all the time and effort she spent with supervising me, Professor Dr. Thomas Elbert and Professor Dr. Heinrich H. Buelthoff for reviewing this thesis and Gabriela Diebold for technical assistance with the data acquisition. I would also like to thank Dr. Douglas Cunningham for his helpful suggestions on the creation of the used stimuli and all the other members of the Max-Planck-Institute for biological Cybernetics, who were always willing to share their expertise with me.

Contents

Abstract

Visual object recognition is important for guiding our interactions within our environment. An important step in visual processing is segregating contours from their background and integrating them into meaningful shapes.

The lateral occipital complex (LOC) in the human brain has been proposed to be primarily involved in the visual analysis of shape. This region is found bilaterally on the lateral surface of the occipital lobe, adjacent to the lateral occipital sulcus, and extends anterior into the posterior and mid fusiform gyrus and into the occipito-temporal sulcus (Grill-Spector, 2000b). The lateral occipital complex is activated more strongly by intact images of objects than by scrambled versions of these images. The lateral occipital complex responds both to familiar and novel shapes, suggesting that this region is involved in an intermediate pre-semantic level of visual processing.

The goal of the present study was to investigate the role of the lateral occipital complex in figure-ground segregation and contour integration of simple geometric shapes by using event-related functional magnetic resonance imaging in human subjects.

To this end, the lateral occipital complex was independently localized in each subject as the set of voxels in the occipito-temporal cortex that shows significantly ($p<10^{-3}$) stronger activation when observers are presented with intact than scrambled images. Then the event-related time-course of the percent MR signal change was computed across subjects in the lateral occipital complex.

The stimuli were constructed by using arrays of Gabor patches. Two types of stimuli were used: a) Random patterns that consisted of randomly oriented Gabor patches and b) contours that consisted of a set of Gabor patches that were aligned to a closed contour and embedded in a background of randomly oriented Gabors.

In the first experiment, we tested whether responses in the lateral occipital complex are stronger for contours than for random patterns. Moreover, we investigated the effect of visual cues, namely stereo and motion in facilitating the integration of local elements into contours. The event-related time-course in the lateral occipital complex revealed stronger activation for simple shapes in comparison to random patterns and showed stronger activation when depth and motion were added as facilitating cues.

In a second set of experiments, we tested how degradation of the stimulus affects responses in the lateral occipital complex. To this end, we manipulated the alignment of Gabor patches used to create the shape contours. Our results showed decreased activation

in the lateral occipital complex for misaligned contours that were difficult to detect from their background.

In summary, our results provide evidence for the involvement of the lateral occipital complex in segregating shapes from their backgrounds and integrating their contours into a whole. Furthermore, our results showed increased activation in the lateral occipital complex when detection of contours is facilitated by visual cues such as stereo and motion. That is, neural responses correlate with our perception of visual shapes.

1. Introduction

1.1 General intention of this study

Representation and perception of the world from the stream of photons that constantly fall onto our retina is a major achievement of our visual system. Visual representations of objects enable us to understand spatio-temporal relationships between objects and ourselves and thus, give us the basis for our behaviour and interactions within our environment.

Traditional psychophysical approaches have proposed several mechanisms to describe how we integrate local image features, for example contours, into coherent shapes (for example Wertheimer, 1912). However, these descriptions remain on a phenomenological level and do not explain how we construct visual perceptions of our world.

Recent neuroimaging techniques allow us to further investigate the neural mechanisms that underlie visual perception. Human functional magnetic resonance imaging studies (Malach et al., 1995) have suggested that the lateral occipital complex (LOC), an area in the occipito-temporal cortex, is involved in processing shape information.

The goal of this thesis was to test whether the lateral occipital complex is involved in the integration of contours into shapes, by using human functional magnetic resonance imaging.

1.2 Shape processing and contour integration

The extraction of visual contours from their background is an important step in the process of perceiving shapes. In our natural environment, we usually encounter objects surrounded by other objects occluding each other rather than in isolation. To detect and recognise a single object, the visual system has to extract its shape information segregated from its background. Furthermore, it has to group object contours into an integrated whole. Once the visual system has segregated contours from its background and integrated them into a coherent shape, further processing, as for example object recognition can take place.

The principles underlying contour integration and figure background segregation have been the target for extensive psychophysical research. To explain the mechanisms of contour integration, a local association field model has been proposed that suggests that

contour elements are locally integrated when their orientation approximately conforms to a similar curve (Field et al., 1993). It has been suggested that similar local processes may be involved in texture segregation (Nothdurft, 1991). That is, segregation of textures occurs due to feature contrasts at the texture borders.

However, psychophysical studies on human subjects have shown that contour integration does not rely only on local field association, but also on global grouping processes (Kovacs & Julesz, 1993). It has been shown that it is easier for subjects to integrate and segregate closed contours than open contours from a cluttered background. This "closed contour superiority effect" cannot be explained by local interactions alone and may reflect the fact, that we encounter objects with closed contours more often than open contours in our everyday life. Thus, we have an advantage in perceiving the type of stimuli we encounter more often in our environment. That is, our visual system is obviously constructed to meet the needs of our daily life.

On a physiological level, previous studies suggest that contour integration and figure-ground assignment take place in early visual areas, namely V1 (for a review: Kovacs, 1996). Orientation-tuned cells in V1 (Hubel & Wiesel, 1968) have horizontal long-range inter-connections (Polat & Sagi, 1994), which could provide a physiological basis for the integration of contour information. These long-range connections occur between neurons with similar orientation tuning and span receptive fields of several degrees (Gilbert & Wiesel 1982). Such interconnections could explain local contour integration in terms of local association fields. However, it is still unknown how the information from local orientation detectors is integrated via long-range interconnections.

1.3 Neural correlates of shape processing

It has been suggested that processing of visual information is performed in a hierarchical manner (Ungerleider & Mishkin, 1982). Starting in the primary visual cortex, we find simple cells that serve as orientation-detectors. Also in V1 we find complex cells that have larger receptive fields than the simple cells and that integrate signal from several simple cells (Hubel & Wiesel, 1968). Studies in humans and monkeys have provided evidence for the involvement of the primary visual cortex in texture segregation based on orientation contrast (Lamme et al., 1992).

However, our visual system is capable to do more than just integrate contour lines and assemble them into a whole shape. At any given timepoint, we usually encounter more than one single object. Objects occlude each other and for us to be able to recognize an

object, our visual system needs to extrapolate the structure of an object. This mechanism becomes obvious when we perceive subjective contours as for example in the Kanizsa illusion (Kanizsa, 1979). In such a case, we see contours even though there is no physical basis for our percept. Electrophysiological investigations in the monkey cortex found that cells in area V2 fire in relation to illusory contours (von der Heydt & Peterhans, 1989).

Perception of occluded objects requires a mechanism that segregates the object contours from their background. Some neurons in area V4 are preferentially activated when a shape is segregated from its background (Desimone & Schein, 1987). Lesion studies in the monkey support this finding. Specifically, ablation of area V4 results in specific perceptual deficits for texture-defined and illusory contours. Thus, processing of illusory contours may depend on several distributed brain structures.

What happens to visual shape information, once it is separated from its background? Cells in the infero-temporal cortex encode representations of moderately complex shapes (Tanaka, 1996), as has been shown in electrophysiological studies of the monkey cortex. Neurons in the posterior infero-temporal cortex, namely area TEO respond to shapes at a specific location. However, neurons in the more anterior regions of the infero-temporal cortex that is in area TE respond to shapes independently of their spatial location. Taken together, these studies suggest that neural information about shapes is integrated across multiple visual areas.

Similarly, recent neuroimaging studies suggest hierarchical visual processing in the human brain. An fMRI study (Lerner, 2001) has found that sensitivity to scrambling of images increases from posterior to anterior brain regions. This finding has been interpreted as evidence for a hierarchical axis along the ventral stream, in which processing of local features gradually develops into global representations of objects.

The process of segregating contours from texture has been investigated using fMRI and pronounced activation in area V4 and TEO in the human cortex has been found (Kastner, 2000). This shows the important role of higher level visual areas in texture segmentation processes.

Brain activity related to object-recognition, that is preferential activation to object images rather than texture patterns, has been described in the lateral occipital complex (Malach, 1995). This region also shows increased fMRI signal when stimulated by illusory contours (Mendola, 1999).

Taken together, previous studies suggest that visual information is processed across different brain regions. Later stages in the visual processing stream integrate information

from earlier areas. In the human brain, the lateral occipital complex has been proposed to serve the purpose of encoding object shape. This thesis intends to investigate the role that this higher order visual area plays in the integration of contours into global shapes.

1.4 The lateral occipital complex and its role in shape processing

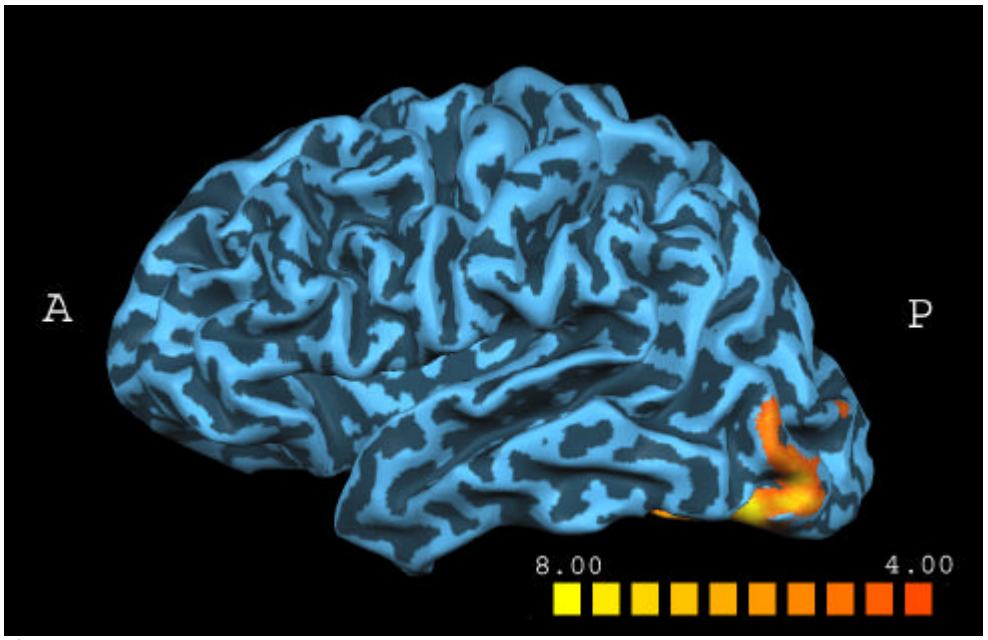

a)

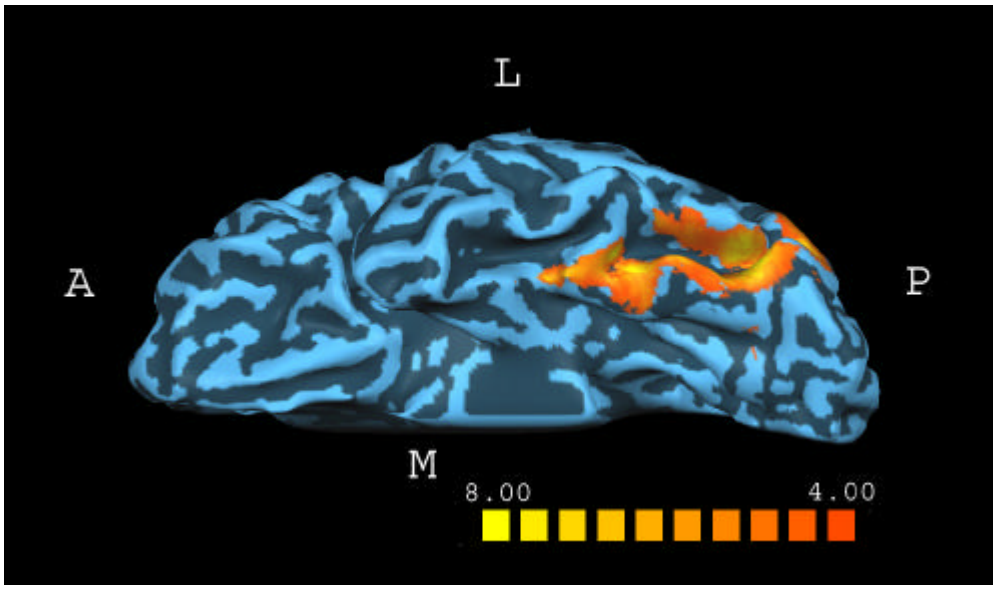

b)

Figure 1.1: Statistical parametric map from a single subject, projected onto a cortical surface reconstruction of the left hemisphere, a) lateral view, b)basal view. Red and yellow coloured areas indicate significantly stronger fMRI activation for intact object images than for scrambled images. A = anterior; P = posterior; L = lateral; M = medial

Anatomically, the lateral occipital complex is bilaterally located posteriorly in the lateral part of the occipital cortex and extends anteriorly into a ventral and a dorsal part, adjacent to the anterior borders of the Brodmann areas 19 and 37 (Malach, 1995). The activation in the lateral occipital complex is not different for familiar and unfamiliar objects. It has been suggested that this region is a homologue for macaque IT that is involved in higher-order visual processing.

In a recent study, the receptive field properties of the lateral occipital complex have been tested (Grill-Spector, 1999). The findings show a differential pattern in two sub-divisions of the lateral occipital complex: There is invariance to changes of size or position in the posterior part of the lateral occipital complex (LO) but even stronger invariance in the anterior parts, the posterior fusiform gyrus (PF/LOa).

Recent studies have investigated the properties of the lateral occipital complex using fMRI in human subjects. Some of these studies provide evidence that there is a center-periphery organization in the lateral occipital complex based on eccentricity maps (Levy et al., 2001). Eccentricity maps are usually found in retinotopic areas and relate to the fact that areas in the retina that are further apart from the fovea are represented in retinotopic brain areas further apart from the foveal representation. According to Levy et al., images of faces are more strongly associated with foveal representation in the lateral occipital complex, whereas images of buildings are more related to peripheral representation. This organisation might reflect the spatial extent of these object categories in everyday life: That is, we usually focus on other people's faces, whereas buildings are often too large to fit into our central view.

Moreover, there is evidence, that the lateral occipital complex encodes shape information independent of the image cues that define the shape. Specifically, similar activations were observed in the lateral occipital complex for grayscale pictures and line drawings of the same objects. Furthermore, similar responses in the lateral occipital complex were observed for shapes defined by luminance, texture or motion (Grill-Spector et al., 1998). These studies suggest that the lateral occipital complex is involved in the processing of the perceived shape rather than simple low-level image feature.

In summary, neural populations in the human lateral occipital complex encode visual information about the perceptual shape structure (Grill-Spector et al., 2000b; Malach et al., 1995). In contrast to earlier visual areas (V1, V2, V3, V3a) the lateral

occipital complex represents objects invariant to their size and position, similarly to macaque infero-temporal neurons (Tanaka, 1996).

1.5 Contour integration in the human lateral occipital complex

The goal of this thesis was to test whether the lateral occipital complex is involved in representing shapes segregated from a background by integrating contours. Our prediction was, that these integrated contours result in activation in the lateral occipital complex that encodes shape information.

In our everyday environment we usually have more information for segregating objects from its surrounding background than in artificial laboratory situations during psychophysical experiments (Gibson, 1979). While images in these experimental conditions often appear on a flat screen, in our everyday life we have depth information about objects because of binocular disparity. That is, in our close environment we can judge how far apart an object is situated and with this additional information we can group object parts together. Depth cues help to understand which parts belong together and thus facilitate contour integration and the segregation from background (Nakayama et al., 1989). In the present study, we used stereo to facilitate contour integration and detection and tested the effect of this visual cue on the responses in the lateral occipital complex.
Another important visual cue in our everyday life is motion: When we explore our world, we find ourselves in a dynamic rather than a static visual environment. Since it was crucial for our ancestors to perceive moving predators before they got too close, our visual system is extremely responsive to moving objects. We instantly group contours together that share the same translation and velocity vector. The integration of motion information and figure-ground segmentation has been investigated in psychophysical studies (Stoner & Albright, 1996). These studies have shown interactions between motion processing and surface segmentation. In our studies we tested whether the lateral occipital complex shows modulated activation when motion cues are added.

In a series of experiments motion and stereo were added to visual contours to investigate, whether facilitation of contour integration by these cues modulates the fMRI signal in the lateral occipital complex. That is, we asked whether the facilitation of contour detection due to additional visual cues results in stronger activations in the lateral occipital complex.

Another important question to be addressed was the following: What happens when it becomes harder to segregate the contours from their background? This might occur,

when the background gets more cluttered or when the contours are less smoothly aligned. Thus, does the activation in the lateral occipital complex correlate with the subject's detection rate? This question was tested in a recent monkey fMRI study by parametrically adding noise to natural images (Rainer et al., 2001). Furthermore, in a human fMRI study, activation in the lateral occipital complex was recorded for masked object images (Grill-Spector et al., 2000a). The duration of exposure was parametrically varied between 20 and 500 milliseconds. A correlation between object naming performance and fMRI signal was observed in the lateral occipital complex, but not in area V1. This suggests that activation in the lateral occipital complex reflects conscious perception of a stimulus. Another human fMRI study supports this view and provides evidence that fMR signal in the fusiform gyrus increases as a linear function of the ability to recognize objects (Bar, 2001).

In sum, this thesis addressed the following questions: a) whether the human lateral occipital complex is involved in processes of contour integration and figure-ground segregation and b) whether visual cues that facilitate contour integration modulate the fMRI response in the lateral occipital complex and c) whether perceptual saliency of a shape is correlated with activation in the lateral occipital complex.

1.6 Contour integration in the lateral occipital complex: Hypotheses

In the first experiment, we compared fMRI responses in the lateral occipital complex between conditions when subjects were presented with contours embedded in a noisy background and when they were presented with random patterns alone. If the lateral occipital complex is involved in contour integration and representation of shape information, then the responses in the lateral occipital complex should be higher for stimuli with embedded contours.

In addition, we tested conditions where additional visual cues, namely depth and motion were added to the contours. We predicted that facilitation of contour integration by these additional visual cues would result in stronger activations in the lateral occipital complex.

A second and third experiment tested whether difficulty in segregating contours from a noisy background modulates the activations in the lateral occipital complex. To this end, we varied the degree of alignment of the local elements used to create contours. We predicted that misalignment of local elements would result in decreased contour detection performance and in lower fMRI responses in the lateral occipital complex. Finally we tested whether additional visual cues that may facilitate the detection of misaligned contours result in better detection performance and stronger responses in the lateral occipital complex.

2. Methods

2.1 Subjects

Thirty-two subjects from the University of Tübingen participated in this study after they have given informed written consent. All had normal or corrected-to-normal vision. Data from three subjects were excluded from analysis due to excessive head movement.

Experiment	N	Male / Female	Mean Age	Right / Left handed
Experiment 1	10 (0)	6 / 4	23.8	9 / 1
Experiment 2	10 (2)	6 / 4	31.7	10 / 0
Experiment 3	9 (1)	2 / 7	25	9 / 0

Table 2.1: Subjects that participated in the three different experiments. N is the number of subjects. The number of excluded subjects is shown in brackets.

2.2 Material

Stimuli used in the LOC localizer scans and in the event-related scans were 250*250 pixel images, resulting in 6.6 degrees of visual angle. To independently localize the LOC we used grayscale pictures of novel and familiar objects as well as scrambled versions of each

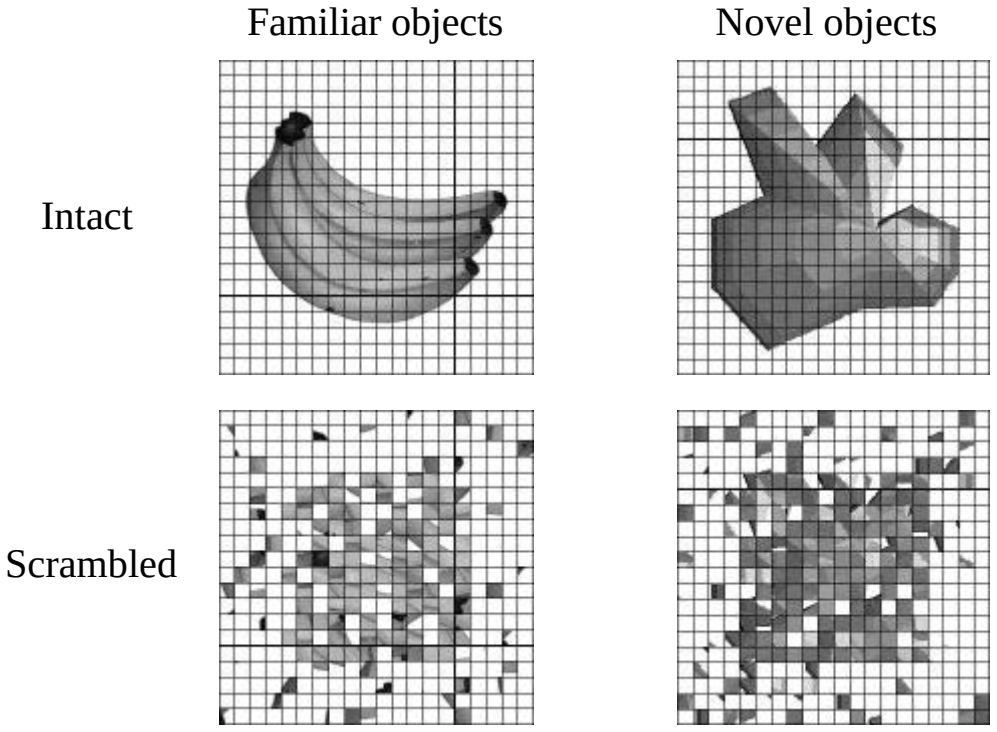

Figure 2.1: Example stimuli from each of the four stimulus conditions in the LOC localizer scan.

set (Figure 2.1). In each condition, 20 different objects were used. The scrambled images, were created by dividing the intact images into a 20 * 20 square grid and then by randomising the positions of each resulting square within each one of three circular regions defined by concentric rings. The grid lines appeared in both the intact and the scrambled images to match these two conditions for spatial frequency.

For the event-related scans we used images consisting of Gabor element arrays. Gabor elements are sinusoidal luminance gratings overlaid with a gaussian envelope function (Figure 2.2).

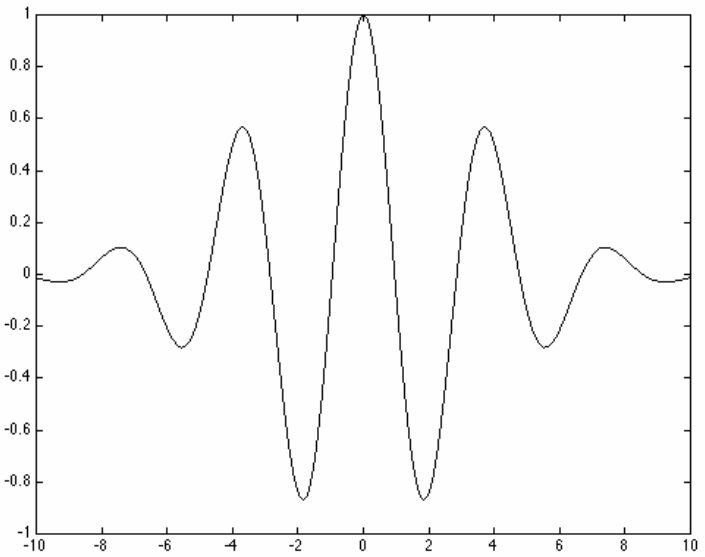

Figure 2.2a: Two-dimensional plot of a Gabor function

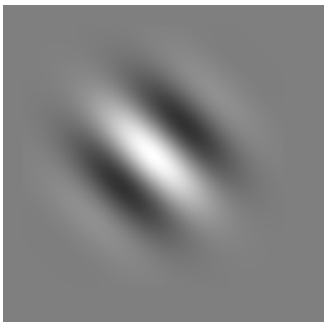

Figure 2.2b: Single Gabor

Images consisted of a 12 * 12 Gabor array, with the elements defined by the following equation:

$$G(x,y) = e^{\frac{-(x^2+y^2)}{2s^2}} (\cos(\frac{2p(\cos(J)x+\sin(J)y)}{p}))$$

G is the gray level at position (x,y). The size of a Gabor element is defined by the σ parameter and was kept constant for all images. A single Gabor had a size of σ = 8 pixels, resulting in a full width of 16 pixels (2σ) at half-height of an element. This equals a visual angle of approximately 0.4 degrees. The period parameter was set to p = 6 pixels.

There were two different classes of stimuli: Gabor arrays that were mere random patterns and arrays that had contours embedded. These contours were produced by aligning and positioning the Gabor elements along a closed path.

To ensure a homogenous distribution of Gabors across the whole field, the field was regarded as a 12*12 grid with the Gabor elements placed into the cells of this grid.

Each cell contained one single element, that is every image contained in total 144 Gabor elements.

The random pattern stimuli were created by randomly positioning the Gabor elements into the grid cells. Orientations of the Gabor patches were randomly assigned.

Contour stimuli were created based on the following procedure:

The contour lines were computed either by combining sine and cosine waves or by connecting Bezier splines with different amounts of connection points to a closed contour (confer Appendix B). These closed contour lines were overlaid with a 12*12 cell grid and the intersections with this grid were extracted. The intersections of each grid square were connected and the centre of the line, which connected the two intersections, was computed. The angle of this line served as orientation parameter θ and the position of the line centre as position parameter for a Gabor patch (Figure 2.3).

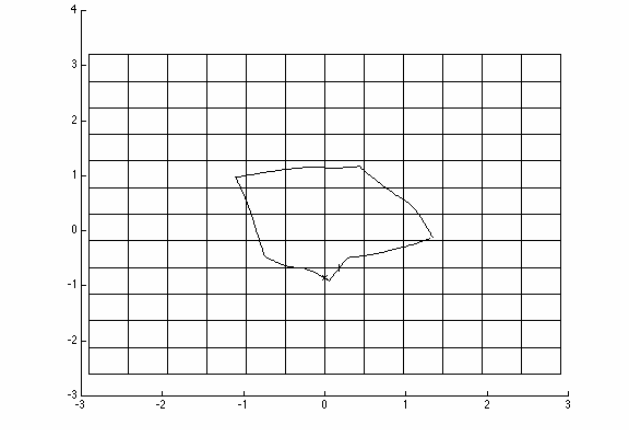

Figure 2.3a: Example of a Bezier spline and an overlaid grid.

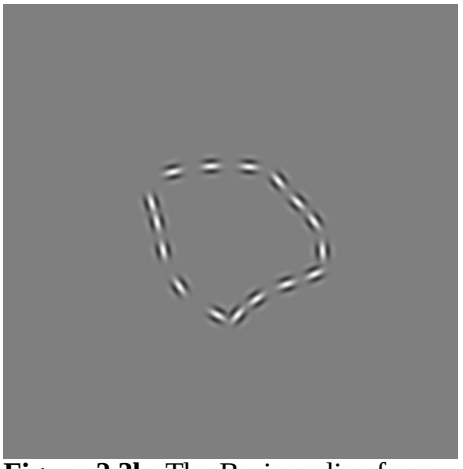

Figure 2.3b: The Bezier spline from Figure 2.3a, rendered with Gabor elements.

To produce salient shapes, two versions of a contour with different sizes were put together, so that the smaller version of the contour was centred within the larger version.

Thus, better detectability of the shapes was achieved. The contours were embedded into randomly oriented Gabor fields as backgrounds.

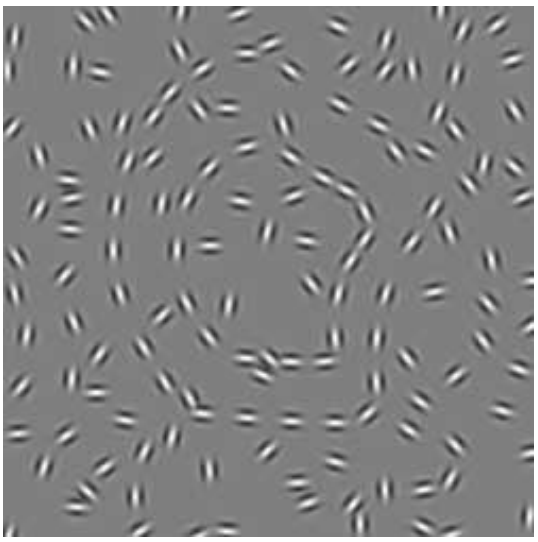

a)

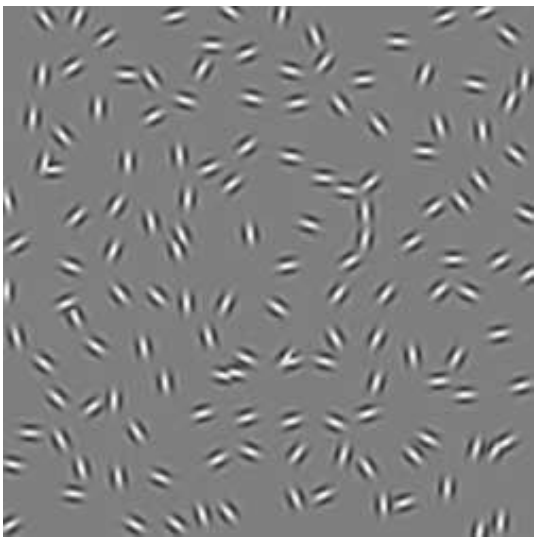

b)

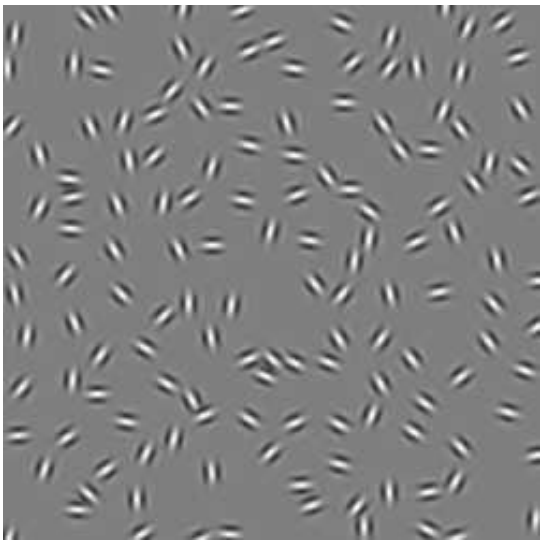

c)

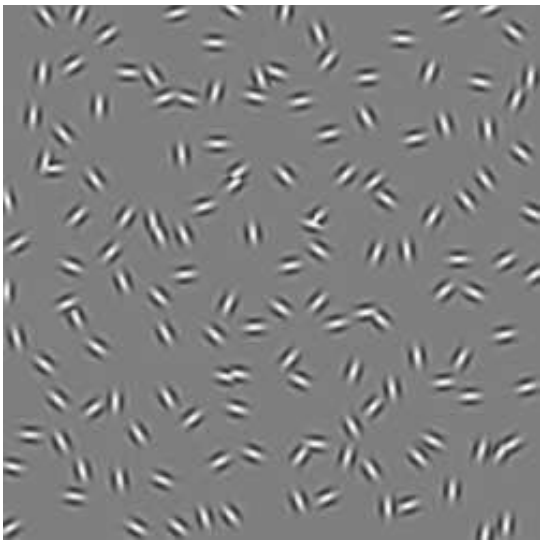

d)

Figure 2.4: Example stimuli used in experiments 1,2 and 3:
a) aligned contour, b) misaligned contour (20-25 degrees, used in experiment 2)
c) misaligned contour (25-30 degrees, used in experiment 3), d) random pattern

In all experiments, we included conditions in which visual cues, that is stereo and motion, were added to the contours and to the random patterns, respectively. For the stimuli in stereo, we rendered the Gabor elements which were part of a closed contour as red-green anaglyphs. Subjects wore red-green-filter glasses during all the scans. The disparity between the red and the green parts of the anaglyphs was 3 pixels. This disparity

elicited the impression that the anaglyphs were in front of the background Gabor elements. As control stimuli we randomly selected Gabor patches within the random patterns and rendered them as red-green anaglyphs in the same way as described above. These patches were selected to match the extension of the contours and the number of Gabor elements, that were part of the contour.

Another visual cue was motion. As before, we added this visual cue to both the contours and the random patterns. Motion was induced by switching between three image frames: The first frame was followed by a second frame with selected Gabor elements shifted by 3 pixels to the right. After that, a last image frame was shown, which was the same as the first.

In experiment 2 and 3 we degraded the contours by adding a random angle to each Gabor element of a closed contour. This random angle was ± 20 to 25 degrees for experiment 2 and ± 25 to 30 degrees in experiment 3. That is, a random angle within these specified ranges was chosen for each single Gabor element in the contour and randomly either added to or subtracted from the element's angle.

For all three event-related experiments, there were different sets of contour stimuli in each condition, so that within a scan, the subjects were not presented with the same contours in two different conditions. Across scans and subjects this assignment of sets to conditions was counterbalanced. That is every set appeared in a certain condition as often as other sets. This counterbalancing ensured that the measured effects were not due to the properties of a specific stimulus set.

2.3 Procedure

2.3.1 Localization of the lateral occipital complex

In all three experiments we localized individually for each subject the lateral occipital complex, that is the set of voxels in the occipito-temporal region that showed stronger activation for intact than for scrambled images of objects (Kourtzi & Kanwisher, 2000a).
To localize the LOC a blocked design was used with sixteen 16-seconds stimulus epochs and interleaved fixation periods of 16 seconds. In the beginning and at the end an 8 seconds fixation period was presented. Each scan lasted for 5 minutes and 36 seconds. Subjects were scanned twice in this LOC localizer scan.
Within each stimulus epoch of 16 seconds 20 pictures of the same type were shown. Each picture was presented for 300 milliseconds, followed by a blank of 500 milliseconds.

Each of the four stimulus types (intact grayscale pictures of familiar objects, intact grayscale images of novel objects and scrambled versions of each set) were presented in different epochs within each scan, in a design that balanced for the order of conditions.
The subjects performed a '1-back' matching task. That is the subjects were instructed to press a button, when they detected two same images in sequence.

2.3.2 Experiment 1

An event-related design with 99 trials per scan was used in this first experiment. Each subject was run in four scans. For each of the six experimental conditions, there were 14 trials per scan and further 14 fixation trials, which were presented interleaved. A new trial began every 3 seconds. The order of presentation was counterbalanced, so that trials from each condition, fixation trials included, were preceded equally often by trials from each other condition. This counterbalancing was applied to all three event-related experiments. Since there were fixation periods of 8 seconds in the beginning of the scan and in the end, the whole scan lasted 5 minutes, 13 seconds.

In each trial the stimulus was presented for 300 milliseconds and was then followed by a fixation point for 2700 milliseconds. The subjects performed a detection task: That is, the subjects were instructed to press a button when they detected a contour and a different button when they did not perceive any contour. The button-response was balanced across

subjects: Five subjects had to press the right button to indicate that they have detected a contour, and another five subjects the left button. Before the scan sessions, subjects were familiarised with the experiment by performing a brief practice session of 56 trials.

In this experiment we employed the following conditions:

1) Fixation: A fixation dot was shown for 3000 milliseconds. Subjects were instructed not to press any buttons. This condition served as a baseline.

2) 2D contours: Displays of randomly oriented and positioned Gabor elements with an embedded contour of aligned Gabor elements.

3) Stereo contours: Displays with the Gabor elements of the contours presented in stereo.

4) Moving contours: In this condition, three image frames were shown, each for 100 milliseconds. The first and the third image were the same, while in the second image frame the Gabor patches of the target contour were shifted to the right.

5) 2D random pattern: The display consisted of randomly positioned and oriented Gabor patches.

6) Stereo random pattern: Randomly positioned and oriented Gabor patches were shown in this condition, with randomly chosen elements presented in stereo.

7) Moving random pattern: Gabors were randomly oriented and positioned, but three frames were shown. In the second frame, some elements were shifted to the right. The number and area of these elements matched that of the moving contours.

2.3.3 Experiment 2

In this experiment we tested the effect of degradation of contours on the responses in the lateral occipital complex. Degradation was achieved by misalignment of the stimuli for 20 to 25 degrees in a random direction. This level of misalignment resulted in detection performance of 70 % correct, based on pilot data from four subjects.

Each scan consisted of 129 trials, with 16 trials of each condition. Timing, trial order and task were the same as in Experiment 1. Each scan lasted for 6 minutes and 43 seconds.

In this experiment, eight conditions were presented:

1) Fixation
2) Aligned 2D contours
3) Misaligned 2D contours
4) Misaligned stereo contours
5) Misaligned moving contours
6) 2D random patterns
7) Stereo random patterns
8) Moving random patterns

2.3.4 Experiment 3

A similar procedure was used as in Experiment 2. The misalignment of Gabor elements was increased to 25-30 degrees in a randomly chosen direction. The 2D, stereo and moving random patterns were all presented in one condition. Previous psychophysical pilot data from four subjects showed a detection rate of 60 % for misaligned 2D displays used in this experiment.

Each scan had 109 trials with each trial lasting for 3 seconds. There were 18 trials per condition and the whole scan lasted for 5 minutes and 43 seconds. As in experiment 1 and 2 this scan was repeated four times.

There were six conditions:

1) Fixation
2) 2D aligned contours
3) 2D misaligned contours: In this condition, the local Gabor elements along the contour line were randomly rotated by 25 to 30 degrees in a random direction.
4) Stereo misaligned contours
5) Moving misaligned contours
6) Random patterns: All random patterns, 2D, stereo and moving were presented in one condition.

2.4 Magnetic Resonance Imaging Acquisition

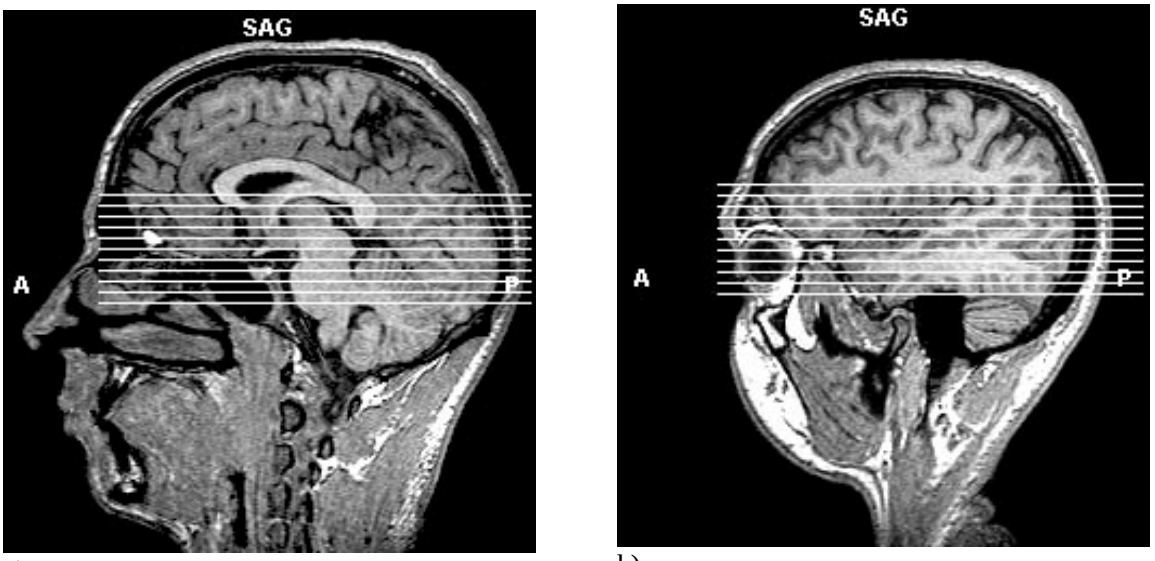

a) b)

Figure 2.5: a) Sagittal and b) lateral transversal view of one subject indicating the position of the selected slices for the fMRI data acquisition.

In all experiments the functional Magnetic Resonance Imaging data were acquired on an 1.5 Tesla Siemens Sonata scanner at the neuroradiology of the University Clinic Schnarrenberg in Tübingen.

Data were collected with a head coil from eleven 5mm-thick axial slices covering the occipital lobe, the temporal lobe and ventral portions of the frontal lobe (Figure 2.5). In-plane resolution was 3.00 x 3.00 mm.

A Gradient-Echo pulse sequence was used, with a TR 2 for the LOC localizer scans, and a TR 1 for the event-related experiments.

2.5 Data Analysis

2.5.1 Analysis of behavioural data

The percent correct responses in Experiment 1 were analysed with a two-way repeated measures ANOVA for Stimulus Structure (contour and random pattern) and Stimulus Format (2D, stereo or moving).

For Experiment 2 we used: 1) A one-way repeated measures ANOVA for Condition (2D aligned contours, 2D misaligned contours, stereo misaligned contours, moving misaligned contours, 2D random patterns, stereo random patterns, moving random patterns). 2) A two-way ANOVA for Stimulus Structure (misaligned contours versus random patterns) and Stimulus Format (2D, stereo or moving). 3) A one-way repeated measures ANOVA for Stimulus structure (2D aligned contours, 2D misaligned contours and 2D random patterns).

Percent correct responses of Experiment 3 were analysed with a one-way repeated measures ANOVA for Condition (2D aligned contours, 2D misaligned contours, stereo misaligned contours, moving misaligned contours, random patterns).

In order to test for significant differences between single factor levels, contrast analysis was conducted on the basis of the degrees of freedom of the according ANOVA. This method was applied in all experiments for both behavioural and fMRI data.

Additionally, d' values were computed from the percent correct data in all the event-related experiments, in order to correct for response biases. This computation was performed based on the formula (Macmillan,N.A., Creelman,C.D., 1991):

$$d' = z(\text{hits}) - z(\text{false alarms})$$

2.5.2 Analysis of functional Magnetic Resonance Imaging data

The fMRI data were analysed using the BrainVoyager 4.4 software package. The functional data were preprocessed. That is, the data were corrected for head movement, high frequencies were temporally filtered and linear trends were removed. 2D functional images were aligned to stereo anatomical data and transformed to Talairach coordinates (confer Appendix C).

To localize the lateral occipital complex in each subject as a region of interest for the analysis of the event-related experiments, functional magnetic resonance data was averaged across two LOC localizer scans. In this averaged time course, voxels were tested for significant stronger response to intact versus scrambled images of objects. These tests were conducted as student t-tests at the significance level of $p < 0.0001$. Significantly responding voxels in the occipito-temporal region were selected as regions of interest for the analysis in all experiments. The Talairach coordinates (Talairach & Tournoux, 1988) were consistent with the ones reported in previous studies (Grill-Spector, 1999).

Time courses of percent signal change were extracted from the lateral occipital complex. The signal was averaged across all voxels in the lateral occipital complex. For each scan we calculated the signal intensity for each trial in each condition based on the hemodynamic response properties for each one of the conditions. Then we averaged across all trials of each condition at each of 10 corresponding time points (seconds) and converted these time courses to percent signal change relative to the fixation trials, by subtracting the averaged signal in the fixation trials from the signal in the experimental conditions.

For all the experiments, first a two-way repeated measures ANOVA was computed for Time (timepoints 0 – 9 from stimulus onset) and Condition (all the experimental conditions within experiment) to justify further analysis on the peak timepoints. The peak timepoints were defined as the timepoints 3,4 and 5 seconds after stimulus onset.

In Experiment 1, a three-way repeated measures ANOVA for Stimulus Structure (contour versus random pattern), Stimulus Format (2D, stereo or moving) and Time (timepoints 3, 4, 5 after stimulus onset) was computed on the averaged time-course of percent signal change.

For Experiment 2, we first computed a two-way repeated measures ANOVA for the within-factor Condition (2D aligned contours, 2D misaligned contours, stereo misaligned contours, moving misaligned contours, 2D random patterns, stereo random

patterns, moving random patterns) and Time (timepoints 3, 4, 5). Then we computed a three-way repeated measures ANOVA for Stimulus Structure (misaligned contour versus random pattern), Stimulus Format (2D, stereo or moving) and Time (3, 4 and 5 seconds after stimulus onset). Finally, a two-way repeated measures ANOVA for Stimulus Structure (2D aligned contour, 2D misaligned contour and 2D random pattern) and Time (3, 4, 5 seconds) was conducted.

In Experiment 3, a two-way repeated measures ANOVA was conducted for Condition (2D aligned contours, 2D misaligned contours, stereo misaligned contours, moving misaligned contours, random patterns) and Time (time-points 3, 4, 5 seconds from stimulus onset).

As for the behavioural data, in all experiments contrast analysis on the basis of the degrees of freedom of the according ANOVA was applied to test for significant differences between single factor levels.

3. Results

3.1 Behavioural Data

3.1.1 Experiment 1

The percent correct responses of the detection task were analysed in a two-way repeated measures ANOVA for Stimulus Structure (contour versus random pattern) and Stimulus Format (2D, stereo and moving). A main effect for stimulus format was found [$F_{(2,18)}$ = 3.8;$p < 0.05$]. Contrast analysis showed significantly [$F_{(2,18)}$ = 7.388; $p < 0.05$] better responses for the conditions in which the visual cues stereo and motion were added. There was no significant main effect for Stimulus Structure [$F_{(1,9)}$ = 0.2; p = 0.8895] and no significant interaction between stimulus Structure and Stimulus Format [$F_{(2,18)}$ = 2.534; p = 0.1072].

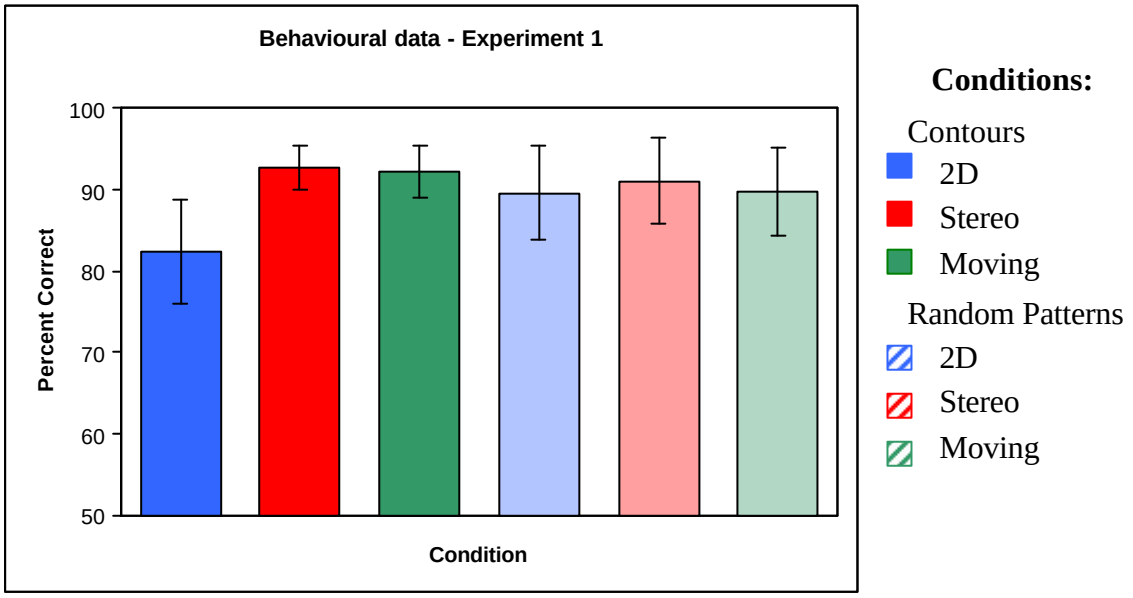

Figure 3.1: Behavioural data for experiment 1: Percent correct responses

Condition	2D	Stereo	Moving
d’	2.2	2.8	2.7

Table 3.1: d’ for the detection responses in Experiment 1.

The results showed that that there was no significant bias for preferentially responding “contour” or “random pattern”. The additional visual cues, that is stereo and motion, led to significantly higher detection rates.

3.1.2 Experiment 2

A one-way repeated measures ANOVA for Condition (2D aligned contours, 2D misaligned contours, stereo misaligned contours, moving misaligned contours, 2D random patterns, stereo random patterns, moving random patterns) was conducted. This analysis showed a significant main effect for Condition [$F_{(6,54)} = 5.458$; $p < 0.001$].

In order to test the effects of Stimulus Structure (contour versus random pattern) and Stimulus Format (2D, stereo and moving), we conducted a two-way repeated measures ANOVA, with the condition of 2D aligned contours excluded.

This analysis showed a significant main effect for Stimulus Format [$F_{(2,18)} = 8.560$; $p < 0.01$] and an interaction between Stimulus Structure and Stimulus Format [$F_{(2,18)} = 8.849$; $p < 0.01$]. There was no significant main effect for Stimulus Structure [$F_{(1,9)} = 0.024$; $p = 0.881$]. Contrast analysis showed significantly higher detection rates for conditions with stereo and motion stimulus than for the 2D stimuli [$F_{(2,18)} = 11.124$; $p < 0.01$].

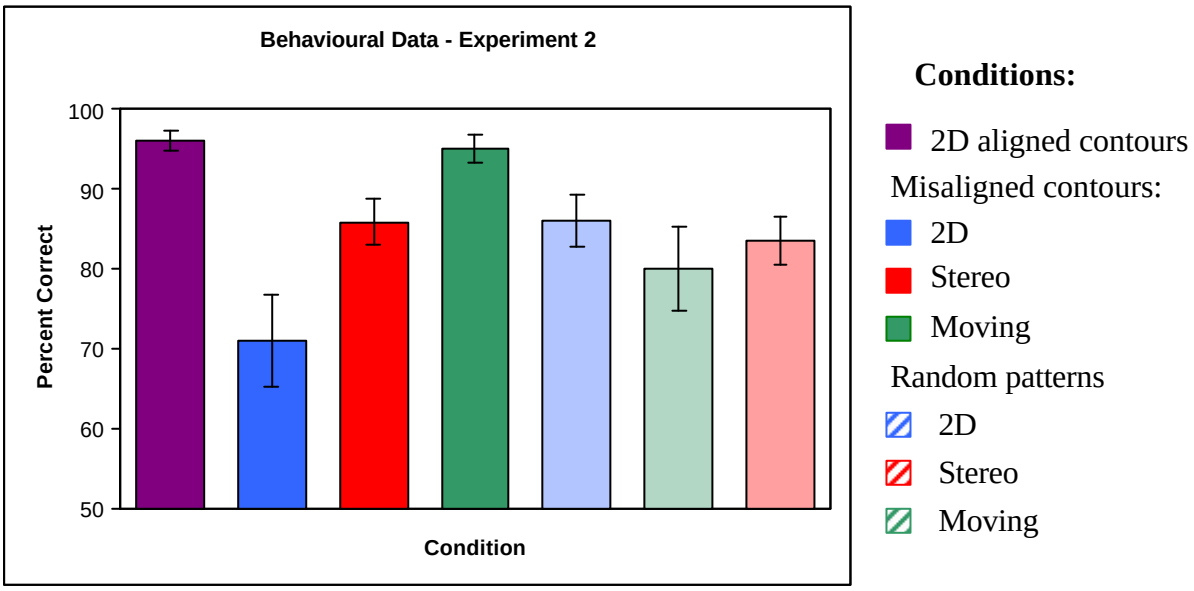

Figure 3.2: Behavioural data for experiment 2: Percent correct responses

Finally, to compare the 2D aligned contours with the 2D misaligned contours and the 2D random patterns, a one-way repeated measures ANOVA was conducted for Stimulus Structure (2D aligned contours, 2D misaligned contours, 2D random patterns). The results showed a significant main effect for Stimulus Structure [$F_{(2,9)} = 7.905$; $p < 0.01$]. Contrast analysis showed significantly higher detection rates for the 2D aligned

contours than for the 2D misaligned contours [$F_{(2,9)}$ = 15.619; $p < 0.001$]. The difference between the percent correct responses for the 2D aligned contours and the 2D random patterns was not significant [$F_{(2,9)}$ = 2.551; $p = 0.128$], but the performance for the 2D misaligned contours was significantly worse than for the 2D random patterns [$F_{(2,9)}$ = 5.546; $p < 0.05$].

Condition	2D aligned	2D misaligned	Stereo	Moving
d’	2.8	1.6	1.9	2.6

Table 3.2: d’ for the detection responses in Experiment 2.

Thus, these data suggest, that the detection rate for the 2D misaligned contours was lower than for the 2D aligned contours. Additional cues (stereo, motion) resulted in higher detection rates. The significant difference in detection rate between the 2D misaligned contours and the 2D random patterns suggests a response bias of the subjects for preferentially responding “random pattern” when 2D misaligned contour or 2D random patterns were shown.

3.1.3 Experiment 3

To analyse the percent correct responses in this experiment, we conducted a one-way repeated measures ANOVA for the within-factor Condition (2D aligned contours, 2D misaligned contours, stereo misaligned contours, moving misaligned contours, random patterns). We obtained a main effect for Condition [$F_{(4,32)} = 9.492$; $p < 0.001$]. A contrast analysis showed significantly higher performance for 2D aligned contours than for 2D misaligned contours [$F_{(4,32)}$ = 24.587; $p < 0.0001$]. Moreover, the detection rate was significantly higher for the stereo misaligned contours and moving misaligned contours than for the 2D misaligned contours plus the moving misaligned contours [$F_{(4,32)}$ = 30.875; $p < 0.0001$]. Contrast comparison showed better responses for the random patterns than for the 2D misaligned contours [$F_{(4,32)}$ = 15.649; $p < 0.001$].

The detection rate for the 2D aligned contours was significantly higher than the rate for the 2D misaligned contours. The responses in the conditions with visual cues (stereo, and motion) are more accurate than the responses to the 2D misaligned contours.

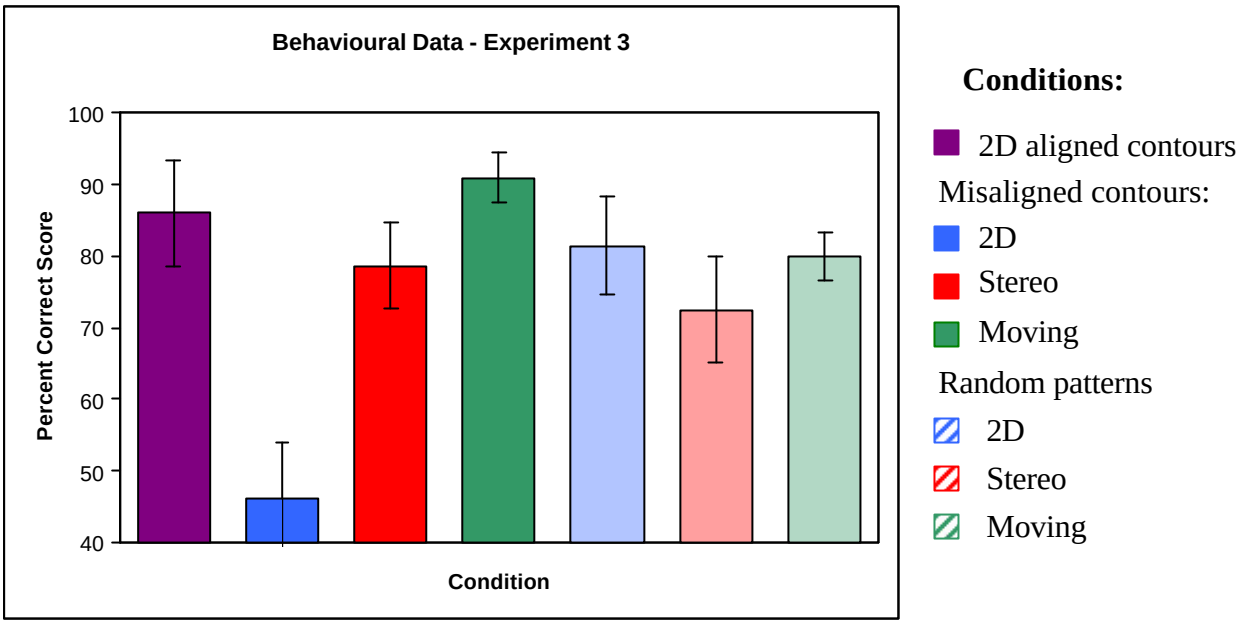

Figure 3.3: Behavioural data for experiment 3: Percent correct responses

Condition	2D aligned	2D misaligned	Stereo	Moving
d’	2.0	0.8	1.7	2.2

Table 3.3: d’ for the detection responses in Experiment 3.

3.1.4 Summary of behavioural data

Analysis of behavioural responses showed two main findings: 1) Higher detection rates for aligned 2D contours than for misaligned 2D contours and 2) Higher detection rates for conditions with additional visual cues (stereo or motion) than for conditions without the cues.

3.2 Functional Magnetic Resonance Imaging data

3.2.1 LOC localizer

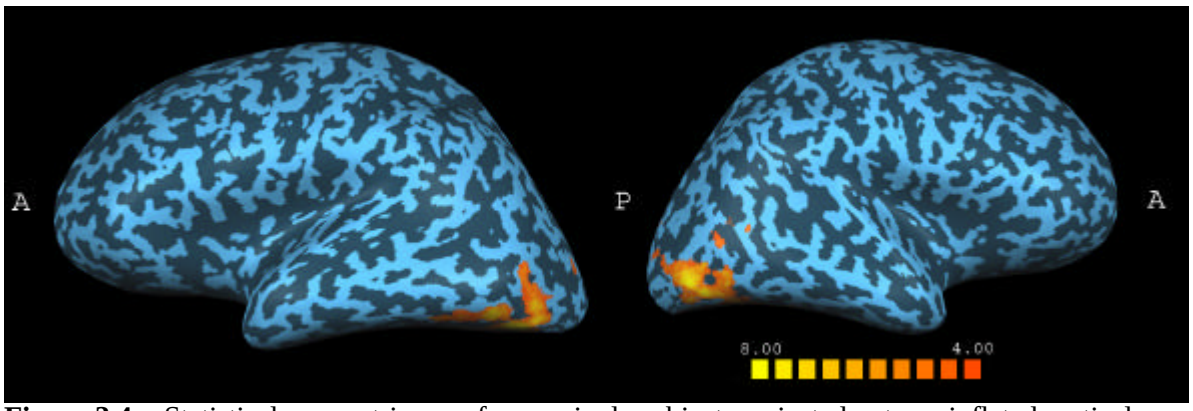

Figure 3.4a: Statistical parametric map from a single subject, projected onto an inflated cortical surface reconstruction of both hemispheres, lateral view. Red and yellow coloured areas indicate significantly stronger fMRI activation for intact object images than for scrambled images. A = anterior; P = posterior.

The averaged data from two LOC localizer scans were used to determine the location of the LOC in each subject. The lateral occipital complex was localized as the set of contiguous voxels in the occipito-temporal cortex that responded significantly ($p < 0.0001$) stronger to intact than to scrambled images of objects.

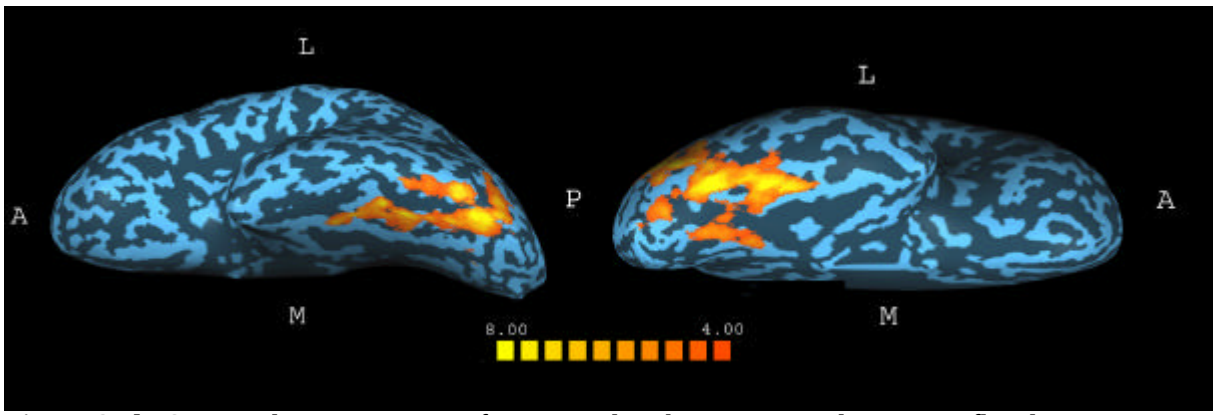

Figure 3.4b: Statistical parametric map from a single subject, projected onto an inflated cortical surface reconstruction of both hemispheres, basal view. Red and yellow coloured areas indicate significantly stronger fMRI activation for intact object images than for scrambled images. A = anterior; P = posterior; L = lateral; M = medial

Table 3.4 summarises the mean Talairach coordinates of the different subregions of the LOC for ten subjects. The obtained coordinates are consistent with data found in previous studies (Levy et al., 2001).

Area	x	y	z
LO Left hemisphere	-40.3 ± 3.1	-74.8 ± 3.4	-7.3 ± 5.5
PFs Left hemisphere	-35.3 ± 4.4	-48.8 ± 4.9	-17.9 ± 3.4
LO Right hemisphere	40.3 ± 2.8	-69.9 ± 4.6	-7.8 ± 4.2
PFs Right hemisphere	33.3 ± 3.6	-44.2 ± 6.4	-17.4 ± 2.8

Table 3.4: Mean Talairach coordinates for the different LOC subregions from 10 subjects. Values are mean ± standard deviation in mm.
LO = lateral occipital region; PFs = posterior fusiform gyrus.

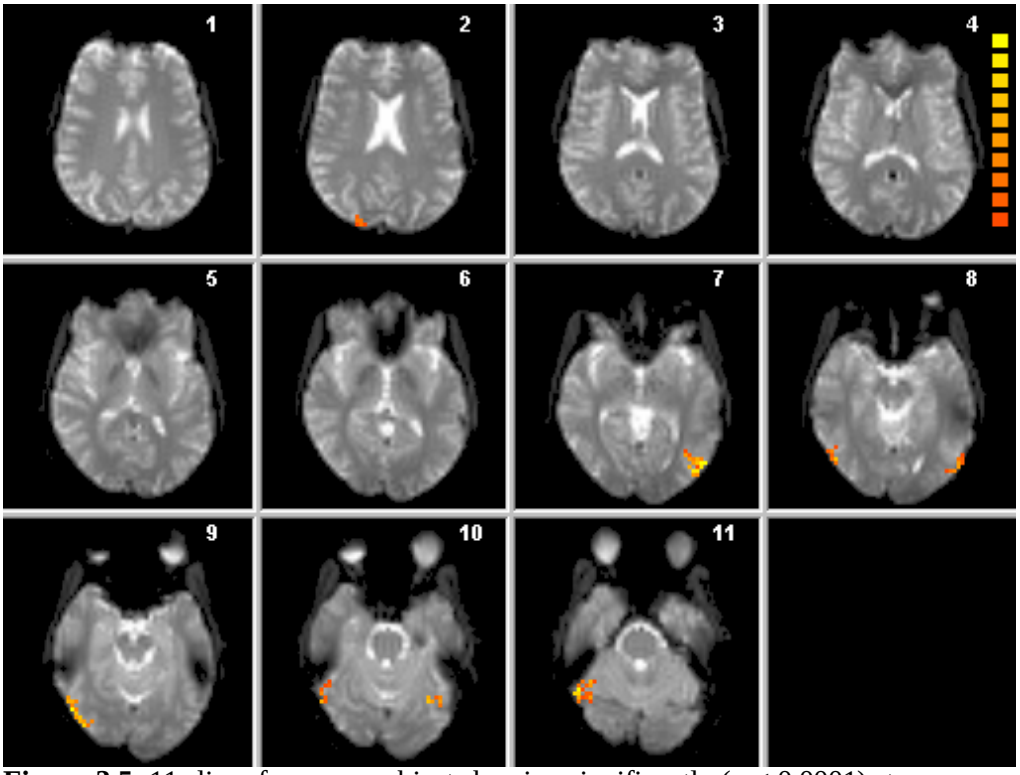

Figure 3.5: 11 slices from one subject showing significantly ($p < 0.0001$) stronger responses for intact versus scrambled images in the LOC localizer scans. Color coding is the same as in Figure 3.4 a and b.

3.2.2 Experiment 1

A repeated measures one-way ANOVA was conducted for Time (timepoints 0 to 9 after stimulus onset) and Condition (2D contours, stereo contours, moving contours, 2D random patterns, stereo random patterns, moving random patterns). It showed a significant main effect for Time [$F_{(9,45)}$ = 16.690; p < 0.0001] and Condition [$F_{(9,45)}$ = 3.291; p < 0.05]. It furthermore showed an interaction between Time and Condition [$F_{(45,81)}$ = 2.384; p < 0.0001]. Contrast analysis between the 2D contours and 2D random patterns at the timepoints [0,1] showed no significant difference [$F_{(45,81)}$ = 0.695; p = 0.4048], but stronger activation for the 2D contours at the signal peak at timepoints [3,4,5] [$F_{(45,81)}$ = 42.454; p < 0.0001]. This result justified further analysis at the signal peak.

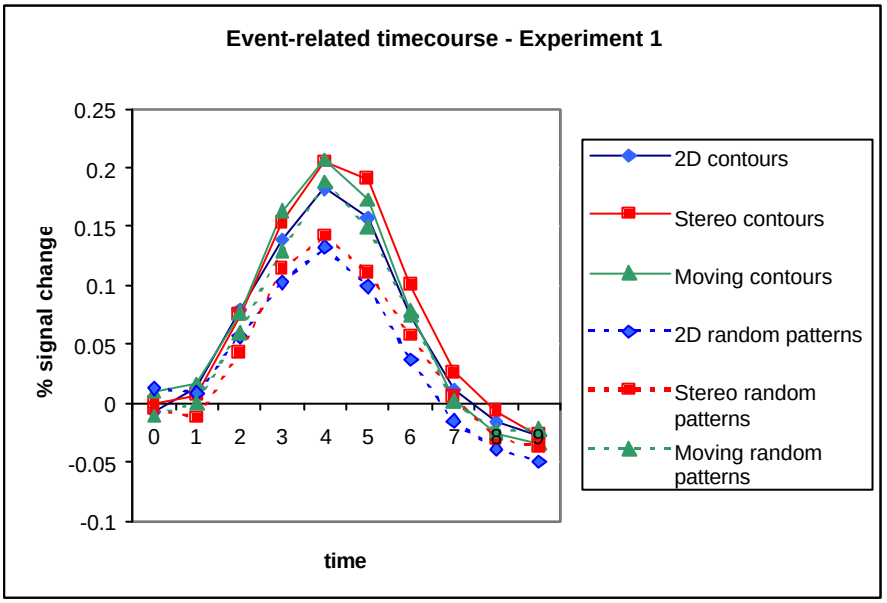

Figure 3.6a: fMRI data for experiment 1: Event-related timecourse in the LOC

A three-way repeated measures ANOVA was applied to the time-course data at the peak timepoints, defined as 3, 4 and 5 seconds after stimulus onset. The ANOVA was conducted for Time (3, 4, and 5 seconds), Stimulus Structure (contour versus random pattern) and Stimulus Format (2D, stereo and moving). Main effects were found for Time [$F_{(2,9)}$ = 4.172; p < 0.05], Stimulus Structure [$F_{(1,9)}$ = 21.792; p < 0.01] and Stimulus Format [$F_{(2,18)}$ = 5.942; p < 0.05]. No interactions occured between Stimulus Format and Stimulus Structure [$F_{(2,18)}$ = 0.846; p = 0.4455], Time and Stimulus Structure [$F_{(2,18)}$ = 1.947;p = 0.1717] or Time and Stimulus Format [$F_{(4,36)}$ = 1.960; p = 0.1215].

Tested with contrast analysis, we found that the 2D stimulus format elicited a significantly weaker fMRI response in the lateral occipital complex than the conditions in which the visual cues stereo and motion were added [$F_{(2,18)} = 8.1$; $p < 0.05$].

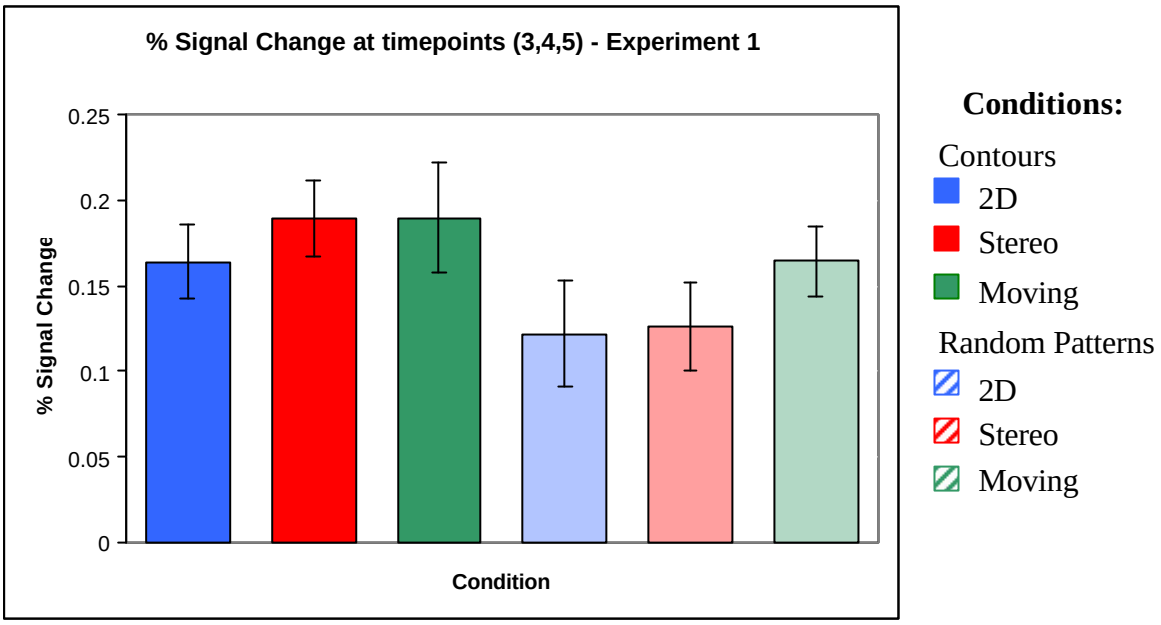

Figure 3.6b: fMRI data for experiment 1: Percent signal change averaged across timepoints (3,4,5)

Taken together, we found stronger activation for contours than for the random patterns. Furthermore, stronger activation in the lateral occipital complex was observed for the conditions where visual cues were added than for 2D contours.

3.2.3 Experiment 2

The lateral occipital complex was defined as the region of interest in this experiment as in Experiment 1. Similar to the first experiment, time-courses of four event-related scans were averaged across scans and then across subjects. Analysis was conducted at the peak of each event-related averaged time-course.

First, we conducted a repeated measures ANOVA for Time (timepoint 0 to 9 after stimulus onset) and Condition (2D aligned contours, 2D misaligned contours, stereo misaligned contours, moving misaligned contours, 2D random patterns, stereo random patterns, moving random patterns) to justify further analysis on the peak timepoints. The main effect for Time was significant [$F_{(9,54)} = 18.662$; $p < 0.0001$], so was the main effect for Condition [$F_{(6,9)} = 2.368$; $p< 0.05$].

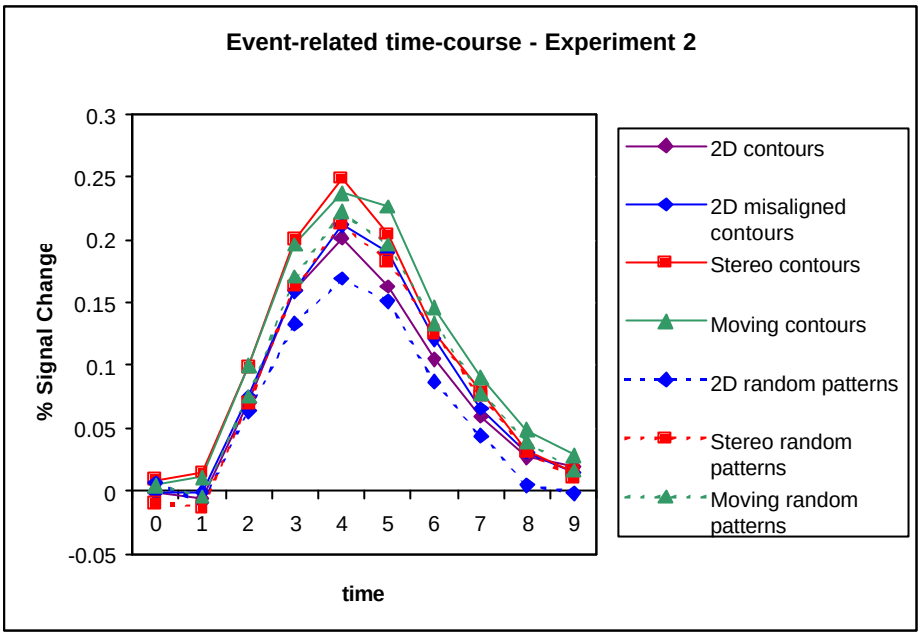

Figure 3.7a: fMRI data for experiment 2: Event-related timecourse in the LOC

Then we conducted a repeated measures ANOVA for Condition (2D aligned contours, 2D misaligned contours, stereo misaligned contours, moving misaligned contours, 2D random patterns, stereo random patterns, moving random patterns) and Time (3, 4, 5 for the peak). There was a clear significant main effect for the factor Condition [$F_{(6,54)}$ = 3.637; $p < 0.01$].

As for the behavioural data, we computed an additional three-way repeated measures ANOVA to differentiate between effects of Stimulus Structure and Format. The ANOVA was computed for Stimulus Structure (contour versus random pattern), Stimulus Format (2D, stereo and moving) and Time (3, 4, 5 for the peak). The conditions with aligned 2D contours were not included into this analysis. The data showed a significant main effect for Stimulus Structure [$F_{(1,9)}$ = 9.784; p = 0.0122] and for Stimulus Format [$F_{(2,18)}$ =5.926; $p < 0.05$]. Contrast analysis between the 2D stimulus format and stereo and motion showed stronger activation in the lateral occipital complex when the visual cues stereo and motion were added than for the 2D stimuli [$F_{(2,18)}$ = 11.588; $p < 0.01$]. There was no significant interaction between Stimulus Structure and Stimulus Format [$F_{(2,18)}$ = 0.144; p = 0.8673]. Furthermore, there was no significant main effect for Time [$F_{(2,18)}$ = 3.506; p = 0.0518] and no significant interaction between Time and Stimulus Structure [$F_{(4,36)}$ = 0.019; p = 0.9807] or Time and Stimulus Format [$F_{(4,36)}$ = 2.393; p = 0.0686].

In a further ANOVA we compared the percent fMRI-signal change for the 2D aligned contours, 2D misaligned contours and the 2D random patterns. The two-way repeated measures ANOVA for Stimulus Structure (2D aligned contour, 2D misaligned contour and 2D random pattern) and Time (3, 4 and 5 seconds) showed no significant main effects, for Stimulus Structure [$F_{(2,18)}$ = 1.894; p = 0.1793] for Time [$F_{(2,18)}$ = 2.687; p = 0.0953].

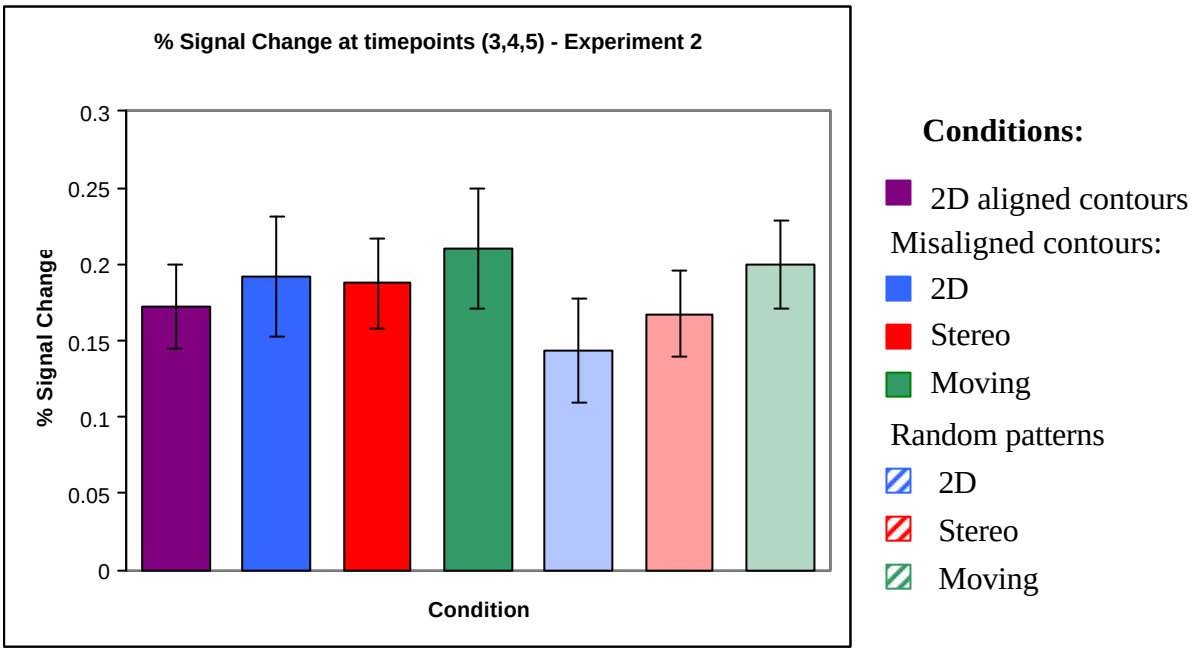

Figure 3.7b: fMRI data for experiment 2: Percent signal change averaged across timepoints (3,4,5)

In sum, the MR signal in the lateral occipital complex was stronger for contours than for random patterns. Furthermore, there was a main effect of stimulus format, suggesting that the activations were stronger, when visual cues such as stereo or motion were added to the contours. No significant difference was found between aligned and misaligned contours.

3.2.4 Experiment 3

We extracted and averaged the time-courses of percent MR-signal change in the same way as in the two previous experiments. A one-way repeated measures ANOVA for Time (0-9 seconds after stimulus onset) and Condition (2D aligned contours, 2D misaligned contours, stereo misaligned contours, moving misaligned contours, random patterns) showed a main effect for time [$F_{(44,9)}$ = 90.771; $p < 0.0001$]. Thus, we were able to selectively analyse the signal at the peak time points.

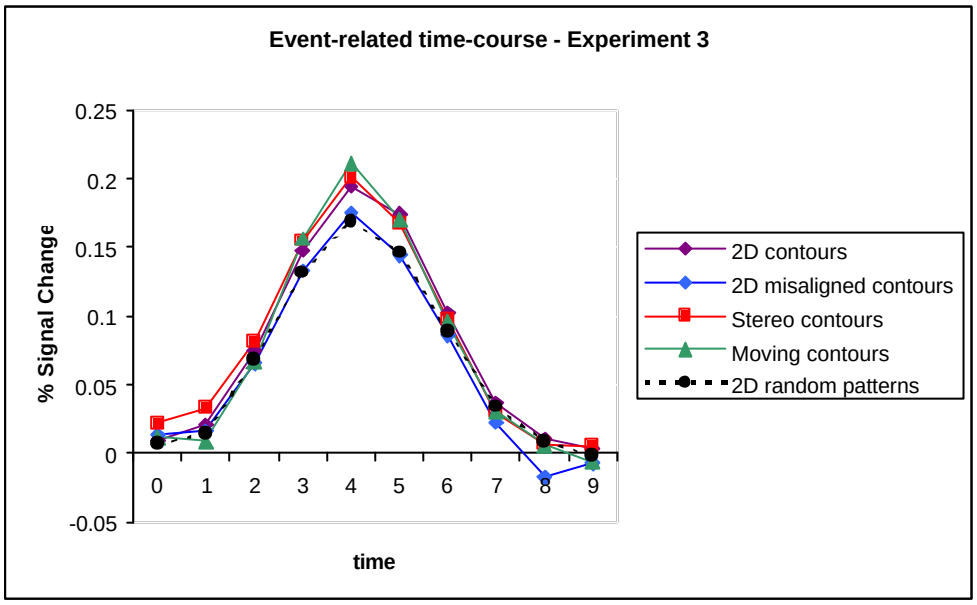

Figure 3.8a: fMRI data for experiment 3: Event-related timecourse in the LOC

We conducted a two-way repeated measures ANOVA for Time (3, 4 and 5 seconds after stimulus onset) and Condition (2D aligned contours, 2D misaligned contours, stereo misaligned contours, moving misaligned contours, random patterns).

The data showed main effects for Condition [$F_{(4,8)}$ = 3.194; $p < 0.05$] and for Time [$F_{(2,32)}$ = 4.607; $p < 0.05$], but no significant interaction between Time and Condition [$F_{(8,16)}$ = 1.216; $p = 0.3042$]. In a contrast analysis, we found significantly stronger fMRI responses in the lateral occipital complex for 2D aligned contours than for misaligned contours [$F_{(4,32)}$ = 4.486; $p < 0.05$]. For the stereo misaligned contours and the moving misaligned contours stronger activation was found than for the 2D misaligned contours [$F_{(4,32)}$ = 8.677; $p < 0.01$].

Taken together, this experiment showed that activation in the LOC were stronger for the 2D aligned contours than for the 2D misaligned contours. The activations were also stronger when visual cues (stereo or motion) were added.

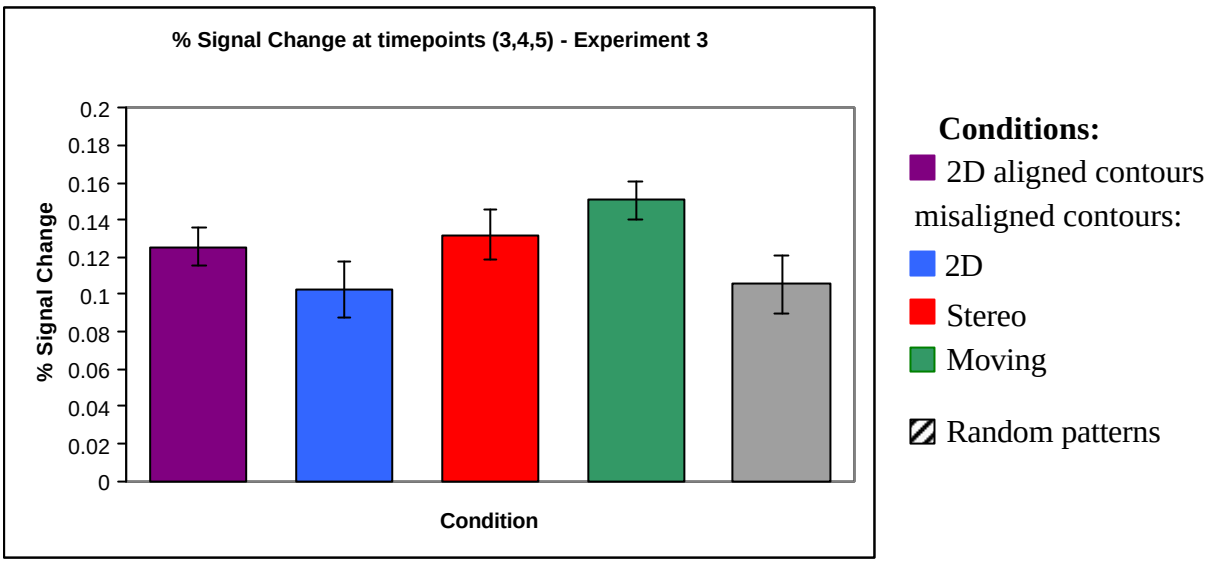

Figure 3.8b: fMRI data for experiment 3: Percent signal change averaged across timepoints (3,4,5)

3.2.5 Summary of fMRI data

This series of experiments showed significantly stronger activations in the lateral occipital complex, when subjects detected a closed contour within a Gabor array than when they were presented with random arrays of Gabor elements. In all three experiments we consistently found stronger fMRI activation in the lateral occipital complex, when we added stereo or motion as visual cues. Degrading of the closed contours by misaligning the Gabor elements results in no significantly different activation in the lateral occipital complex for Experiment 2. However, when the amount of misalignment was increased in Experiment 3 activations in the lateral occipital complex were stronger for the aligned 2D contours than for the misaligned 2D contours.

4. Discussion

4.1 Interpretation of functional magnetic resonance data

The goal of our studies was to investigate the role of the lateral occipital complex in the integration of contours. To this end, we measured the blood oxygenation level dependent (BOLD) response in the human brain using fMRI.

When we refer to the BOLD response as measured brain activity, one has to be aware that we assume that changes in deoxy-hemoglobin blood concentration in cerebral blood vessels are caused by an increase of energy requirements in neuronal tissue. The exact mechanisms that underlie this relationship are still not fully understood. A recent study that combined fMRI with electrophysiological techniques on the monkey cortex suggests strong coupling between the BOLD signal and local field potentials (Logothetis, 2001). These results suggest that the BOLD contrast is linked to incoming input into an area rather than to neuronal output.

In this series of experiments, we acquired fMRI data in an event-related design. This type of design presupposes that the fMRI signal of single trials add in an approximately linear fashion. Previous methodological studies support this assumption (Boynton et al., 1996; Dale & Buckner, 1997) and justify the application of this method.

4.2 Shape Processing in the lateral occipital complex

The integration of contours and their segregation from their background is necessary to be able to extract object shape information from our environment. The lateral occipital complex has been proposed to be primarily involved in encoding shape information (Grill-Spector et al., 2000b). In our first experiment, we tested whether the lateral occipital complex is involved in the integration of contours into simple shapes.

Our findings show significantly stronger activation in the lateral occipital complex for contours versus random patterns. The stimuli used as contours and as random patterns shared common properties, that is same overall luminance level, the same distribution and amount of local elements. Thus, the difference in activation in the lateral occipital complex cannot be explained by the difference in visual low-level features of the used stimuli. This suggests that neural populations in the lateral occipital complex are involved in the process of contour integration and segregation from its background. However, the present data can not conclusively show at what stage of processing the lateral occipital complex is

involved. Previous electrophysiological studies suggest that the integration of contours takes place in visual areas as early as the primary visual cortex (Gilbert & Wiesel, 1982).

A recent human lesion study supports this view. Specifically, contour integration was preserved but processing of occluded shapes was disturbed in a patient with visual agnosia after bilateral ischemia of the occipital cortex and parts of the temporal lobes (Giersch, Humphreys, 2000). This dissociation suggests that integration of contours occurs at an early stage of visual processing and representation of shape information may be processed in higher-level areas.

Therefore, it seems likely that the lateral occipital complex encodes a representation of the global shape that is constructed from local Gabor elements in earlier visual areas. Thus, activation in the lateral occipital complex represents the product from earlier stages of visual computation. This interpretation is consistent with human fMRI studies that show that the lateral occipital complex is involved in encoding shape rather than low-level contour information (Kourtzi, Kanwisher, 2000). This is also consistent with shape processing in area TE in the monkey cortex (Tanaka 1996), for which the lateral occipital complex has been proposed to be a homologue (Malach et al., 1996). A columnar organization has been described in area TE.That is, neighbouring columns in area TE encode similar stimulus features (Fujita, 1992). Considering the size of area TE, the number of columnar modules that encode different shape features are estimated to 1300 (Tanaka, 1996). These modules are proposed to represent prototypes of shapes. Combined activation of these modules could be a way to represent objects. These findings are consistent with recent models of object recognition (Biederman, 1987, Riesenhuber & Poggio, 2000). However, it is still unclear whether such a system is capable of processing our rich visual environment (Logothetis, 1995).

4.3 Processing of visual cues in the lateral occipital complex

Psychophysical studies suggest that additional three-dimensional and motion information about a visual scene facilitate figure-ground segregation (Nakayama et al., 1989). Therefore, in this study we added stereo and motion to the contours to test, whether facilitation of contour integration modulates the fMRI signal in the lateral occipital complex.

Detection performance in all three experiments was increased by stereo and motion cues. That is, it was much easier for subjects to detect contours when these cues were added in comparison to the conditions without the cues, in particular when contours were degraded, as in experiment 2 and 3. Activations in the lateral occipital complex were significantly stronger when local Gabor elements of the stimulus were presented in depth or with motion cues.

These findings suggest that activation in the lateral occipital complex is correlated with detection performance, which is consistent with studies suggesting a correlation between object recognition performance and activation in the lateral occipital complex (Grill-Spector et al., 2000a; Bar et al., 2001).

One possible interpretation for our findings that activation in the lateral occipital complex was increased when motion or depth were added to contours is that these features facilitate shape detection and result in stronger activation in the lateral occipital complex. However, it could be argued, that this increase of activation in the lateral occipital complex is the result of additional image information associated with these visual cues. There was no interaction between stimulus structure and stimulus format in experiments 1 and 2. This suggests that activation in the lateral occipital complex for depth and motion stimuli was similar for both the contours and the random patterns. It may be argued that additional visual cues in a stimulus increase the MR-signal in the lateral occipital complex regardless whether contour detection is facilitated or not. This could be an explanation for our results. However, it could also be argued that when motion or depth are added to some elements of a random pattern, these elements are grouped into a surface. It is possible that surface informationis also processed. Thus responses in the lateral occipital complex for stereo and moving random patterns may be due to processing of surface information in these displays.

Finally, it is important to note that previous studies have suggested cue-invariance to luminance, texture and motion defined shapes in the lateral occipital complex (Grill-Spector, 1998). However, in our studies we found evidence that signal in the lateral occipital complex is modulated by stereo and motion. In these previous studies the subjects

passively viewed pictures of familiar objects. In our studies, the subjects had to detect a contour in a cluttered background. The task was designed so that the subjects' performance was not at ceiling. One possible explanation for these findings is that in our experiments, motion and stereo robustly increased detection rate and this may have resulted in stronger activation in the lateral occipital complex.

4.4 Processing of degraded visual shape information in the lateral occipital complex

To show whether the level of difficulty in contour integration modulates the MR-signal in the lateral occipital complex, we degraded the contours used as stimuli by misaligning the local Gabor elements.

In experiment 2, we found that detection performance for degraded stimuli was significantly lower than for aligned contours or contours that were presented with stereo or motion. However, the detection rate for the misaligned 2D contours was still at a high level, namely 71 percent correct. Brain activation in the lateral occipital complex was not significantly different for the misaligned 2D contours and for the aligned 2D contours. Thus, neural populations in the lateral occipital complex did not significantly differ in their response to degraded and non-degraded contours.

In a further experiment, that is Experiment 3, we increased the level of difficulty. Average detection performance of the subjects was 46 percent. The fMRI data from the lateral occipital complex showed significantly stronger response for the aligned 2D contours than for the misaligned 2D contours. Thus, the fMRI-signal in the lateral occipital complex correlates with detection performance for contours.

Moreover, when we added visual cues to the degraded contours, we found improved detection performance and stronger fMRI responses in the lateral occipital complex than for conditions without visual cues.

4.5 Future directions

We found evidence for a decrease of brain activity in the LOC when stimuli were degraded for one difficulty level of detection, but not for an easier level. This raises the following question: What is the relation between detection performance and activation in the lateral occipital complex like? Is this function linear or rather non-linear, resembling the psychophysical detection curve, as it has been proposed in fMRI studies (Grill-Spector,

2000a) and recent electro-physiological studies (Keysers, 2001). The latter study compared human psychophysical performance on a detection task of rapid serial visual presentation with the firing rate of single cells in the macaque temporal cortex. The findings show a similarity between the performance of human observers as a function of presentation time and single cell recordings in the monkey anterior superior temporal sulcus.

To further test the correlation between detection performance and brain activation in the lateral occipital complex, further studies where the amount of contour misalignment is parametrically varied will be required.

Another approach for investigating the link between perception and activation in the lateral occipital complex could be to investigate the effect of perceptual learning. As we have described before, the lateral occipital complex is equally activated for familiar and novel objects, but this might be true for images that are simple to perceive. Once we increase the difficulty of detection in order to allow learning of shapes to facilitate perception, we may observe modulation of activation in the lateral occipital complex.

Finally, further analysis of fMRI responses in earlier visual areas is needed to test how stimulus properties are processed across different visual areas. Separate analysis of sub-divisions in the lateral occipital complex could provide insights on how processes that relate to integration of visual cues are distributed along this brain region.

4.6 Conclusions

The present study showed that the human lateral occipital complex is involved in the integration of contours and segregation from their background. It was furthermore shown that visual cues such as stereo and motion increase activation in the lateral occipital complex, and that perceptual degradation of the stimulus decreases brain activation in the lateral occipital complex. These findings suggest that activation of the lateral occipital complex is coupled with perceptual performance and that neural populations in the lateral occipital complex are involved in the perception of visual shapes.

5. References

Bar, M., Tootell, R.B.H., Schacter, D.L., Greve, D.N., Fischl, B., Mendola, J.D., Rosen, B.R., Dale, A.M. (2001). Cortical mechanisms specific to explicit visual object recognition. *Neuron, 29*, 529-535.

Biederman, I. (1987). Recognition-by-components: a theory of human image understanding. *Psychological Reviews, 94*, 115-147.

Boynton, G.M., Engel, S.A., Glover, G.H., & Heeger, D.J. (1996). Linear systems analysis of functional magnetic resonance imaging in human V1. *Journal of Neuroscience, 16*, 4207-4221.

Brainard, D. H. (1997). The Psychophysics Toolbox, *Spatial Vision,* 10, 433-436.
Buckner, R.L., Goodman, J., Burock, M., Rotte, M. Koutstaal, W., Schacter, D., Rosen, B,

Dale, A.M., Buckner, R.L. (1997). Selective averaging of rapidly presented individual trials using fMRI. *Human Brain Mapping*, 5, 329-340.

Dale, A.M. (1998). Functional-anatomic correlates of object priming in humans revealed by rapid presentation event-related fMRI. *Neuron, 20*, 285-296.

Desimone, R., Schein, S.J. (1987). Visual properties of neurons in area V4 of the macaque: Sensitivity to stimulus form. *Journal of Neurophysiology, 57*(3), 835-868.

Fujita, I., Tanaka, K., Ito, M., Cheng, K. (1992). Columns for visual features of objects in monkey inferotemporal cortex. *Nature, 360*, 343-46.

Gibson, J.J. (1979). *The ecological approach to visual perception.* Boston: Houghton Mifflin.

Giersch, A., Humphreys, G.W., Boucart, M., Kovacs, I. (2000). The computation of occluded contours in visual agnosia: Evidence for early computation prior to shape binding and figure-ground coding. *Cognitive Neuropsychology, 17(8),* 731-759.

Gilbert, C.D., Wiesel, T.N. (1982). Clustered intracortical connections in cat visual cortex. *Society for Neuroscience Abstracts, 8,* 706.

Glassner, A.S., (1990). *Graphics Gems.* Cambridge: Academic Press.

Grill-Spector, K., Kushnir, T., Hendler, T., Edelman, S., Itzchak, Y., Malach, R. (1998). Cue-invariant activation in object-related areas of the human occipital lobe. *Neuron, 21,* 191-202.

Grill-Spector, K., Kushnir, T., Edelman, S., Avidan, G., Itzchak, Y., Malach, R. (1999). Differential processing of objects under various viewing conditions in the human lateral occipital complex. *Neuron, 24,* 187-203.

Grill-Spector, K, Kushnir, T, Hendler, T, Malach, R (2000a). The dynamics of object-selective activation correlate with recognition performance in humans. *Nature Neuroscience, 3,* 837-843.

Grill-Spector, K., Kourtzi, Z., Kanwisher, N. (2000b). The lateral occipital complex and its role in object recognition. *Vision Research, 41,* 1409-1422.

Hubel, D.H., Wiesel, T.N. (1968). Receptive fields and functional architecture of monkey striate cortex. *Journal of Physiology, 195,* 215-243.

Kanizsa, G. (1979). *Organization in vision: Essays on Gestalt perception.* New York: Praeger.

Kastner, S., De Weerd, P., Ungerleider, L.G. (2000), Texture segregation in the human visual cortex: A functional MRI study. *Journal of Neurophysiology,* 83(4), 2453-2457.

Keysers, C., Xiao, D.K., Foldiak, P., & Perrett, D.I. (2001). The speed of sight. *Journal of Cognitive Neuroscience, 17*, 90-101.

Kourtzi, Z., Kanwisher, N. (2000a). Cortical regions involved in perceiving shape. *Journal of Neuroscience, 20(9),* 3310-3318.

Kourtzi, Z., Kanwisher, N. (2000b). Processing of object structure versus contours in the human lateral occipital complex. *Society for Neuroscience Abstracts, 30,* 22.

Kovacs, I (1996). Gestalten of today: early processing of visual contours and surfaces. *Behavioural Brain Research, 82*, 1-11.

Kovacs, I., Julesz, B. (1993). A closed curve is much more than an incomplete one: Effect of closure In figure-ground segmentation. *Proceedings of the National Academy of Science USA, 90*, 7495-7497.

Lamme, V.A., Van Dijk, B.W., Spekreijse, H. (1992). Texture segregation is processed by primary visual cortex in man and monkey. Evidence from VEP experiments. *Vision Research,* 32 (5), 797-807.

Lerner, Y., Hendler, T., Ben-Bashat, D., Harel, M., Malach, R. (2001). A hierarchical axis of object processing stages in the human visual cortex. *Cerebral Cortex, 11*, 287-297.

Levy, I., Hasson, U., Avidan, G., Hendler, T., Malach, R. (2001). Center-periphery organization of human object areas. *Nature Neuroscience, 4(5)*, 533-539.

Logothetis, N, Sheinberg, D.L. (1995). Visual object recognition. *Annual Reviews of Neuroscience, 19,* 577-621.

Logothetis, N., Pauls, J., Augath, M., Trinath, T., & Oeltermann, A. (2001). Neurophysiological investigation of the basis of the fMRI signal. *Nature, 412,* 150-157.

Macmillan, N.A., Creelman, C.D. (1991). *Detection Theory: A User s Guide.* Cambridge: Cambridge University Press.

Malach, R., Reppas, J. B., Benson, R. B., Kwong, K. K., Jiang, H., Kennedy, W. A., Ledden, P. J., Brady, T. J., Rosen, B. R., & Tootell, R. B. H. (1995). Object-related activity revealed by functional magnetic resonance imaging in human occipital cortex. *Proceedings of the National Academy of Science USA, 92,* 8135-8138.

Mendola, J.D., Dale, A.M., Fischl, B., Liu, A.K., Tootell, R.B.H. (1999). The representation of real and illusory contours in human visual areas revealed by fMRI. Journal of Neuroscience, 29, 8560-8572.

Nakayama, K. Shimojo, S., Silverman, G.H. (1989) Stereoscopic depth: its relation to image segmentation, grouping and the recognition of occluded objects. *Perception, 18,* 55-68.

Polat, U., Sagi, D. (1994). The architecture of perceptual spatial interactions. *Vision Research, 34,* 73-78.

Rainer, G., Augath, M- Trinath, T., Logothetis, N.K. (2001). Nonmonotonic noise tuning of BOLD fMRI signal to natural images in the visual cortex if the anesthetized monkey. *Current Biology, 11,* 846-854.

Riesenhuber, M., Poggio, T. (2000). Models of object recognition. *Nature Neuroscience, 3(Suppl),* 1199-1204.

Stoner, G.R., Albright, T.D. (1996). The interpretation of visual motion: Evidence for surface segmentation mechanisms. *Vision Research, 36(9),* 1291-1310.

Talairach, J., Tournoux, P. (1988). *Co-planar stereotaxic atlas of the human brain.* New York: Thieme

Tanaka, K. (1996). Inferotemporal cortex and object vision. *Annual Review of Neuroscience, 19*, 109-139.

Ungerleider, L.G., Mishkin, M. (1982). Two cortical visual systems. In D.G. Ingle, M.A. Goodale, & R.J.Q. Mansfield (Eds.), *Analysis of visual behaviour* (pp 549-586). Cambridge, MA: MIT Press.

von der Heydt, R., Peterhans, E. (1989). Mechanisms and geometrical illusions. I. Lines of pattern discontinuity. *Journal of Neuroscience, 9(5)*, 1731-1748.

Wertheimer, M. (1912). Über das Sehen von Scheinbewegungen und Scheinkorporen. *Zeitschrift für Psychologie, 61*, 463-485.

Appendix

Appendix A.: Experimental set-up (supplementary information)

Stimuli were generated on a G4 Macintosh Computer, using the PsychToolbox extensions for Matlab (Brainard, 1997). They were projected into the MR scanner room by a NEC MT1050 LCD projector with a frame rate of 60 Hz and a pixel resolution of 1024 x 768. The light beams from the projector fell onto a transparent screen mounted on the head-coil. A mirror behind the screen, which was tilted by 45 degrees, reflected the images into the subject's eyes. Since the images had to be projected into the magnet's bore, the maximum field of view was limited. With our set-up, the maximum vertical field of view was 11 degrees of visual angle, and the maximum horizontal field of view was 22 degrees of visual angle. The extension of our visual stimuli was 250 x 250 pixels, which resulted in a visual angle of 6.6 degrees of visual angle.

For the event-related experiments, the mean luminance level was 450 cd/m^2, which was measured with a calibrated Graseby Optronics photometer, model type 370.

During the whole scan session, subjects held two buttons in their hands, one in each hand. Their button presses were recorded via fibre-optic cables with the stimulus-presenting computer.

Appendix B.: Construction of contour stimuli

To ensure sufficient variety for our closed contour stimuli, two approaches were used for their creation:

1) Combination of sine wave functions:

For this, x- and y-coordinates were created by the following algorithm (using Matlab-like syntax):

```
for  i = 1:360
        x(i) = functionA(i)
        y(i) = functionB(i)
end
```

For example

```
for  i = 1:360
        x(i) =  sin (i* pi/180) * sin(i) * pi/180 + 6.5) ^ 4 + 2);
        y(i) = 1.4 * cos(i* pi/180)*(sin(i+90)*pi/180 + 6.5) ^ 3 );
end
```

would create the following shape:

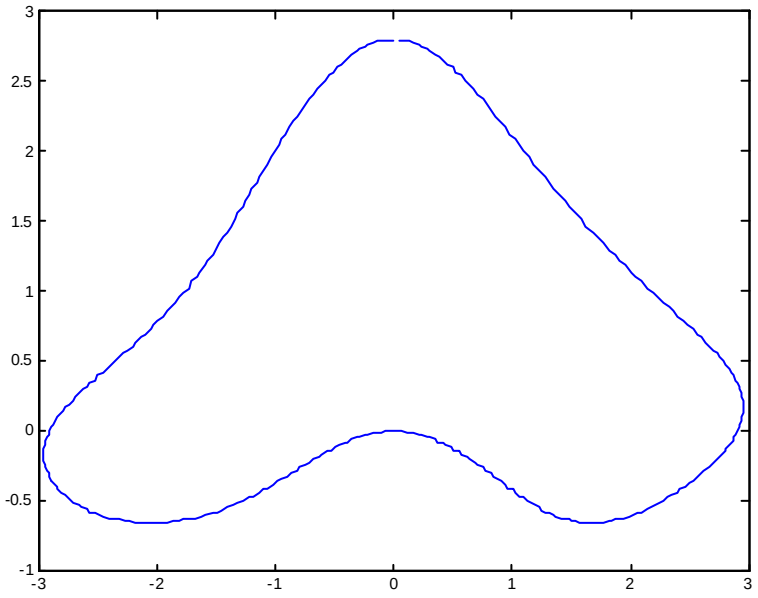

Figure B.1: Combination of sine wave functions generate a closed contour.

Closed contours were generated with the limitation not to have too pointy edges.

2) Bezier curves:

A second approach to generate closed contours was to define a certain number of points and to connect these point with random Bezier curves. The number of points ranged for these studies between 3 and 10. Bezier curves connect two points and demand two further points which control the curves path (Glassner,1990). The following figure shows an example of a Bezier curve connecting two points.

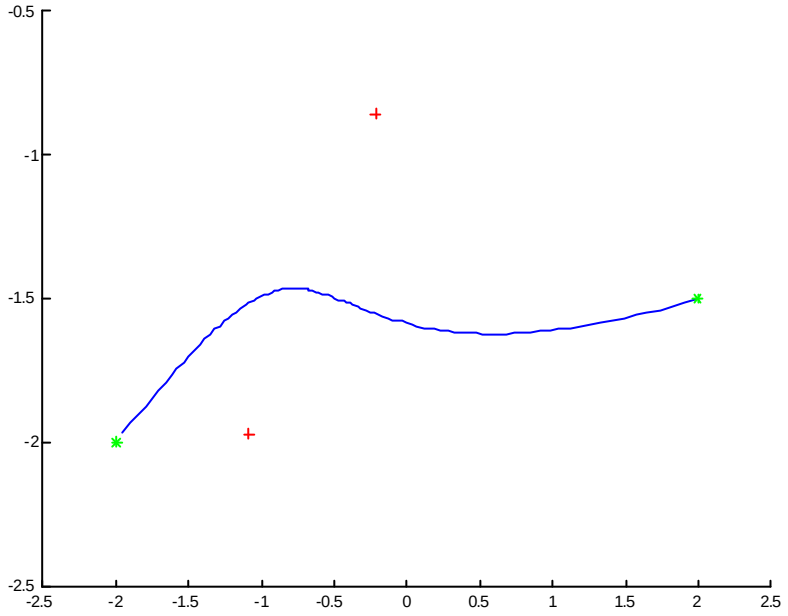

Figure B.2: Bezier curve connecting the two green points,
The red points control the curvature.

By defining more than points which are to be connected, closed contours are generated (see for an example figure 2.3a).

For all our experimental stimulus sets the number of contours generated by the two different approaches were matched across conditions.

Appendix C.: Processing steps in the fMRI data analysis

The analysis of the fMRI data required several steps of pre-processing (Figure A.1 summarises the stages of pre-processing):

1) Pre-processing of functional MR data

The functional T2*-weighted data acquired during the experimental scans underwent the following stages of pre-processing:

a) Slice scan time correction: We gathered functional MR-data from 11 axial slices. In the event-related scans with TR = 1, there was a temporal delay of 91 milliseconds between the acquisition of data from two neighbouring slice planes. In order not to lose statistical power in these scans, correction for inter slice scan times was applied.

b) Motion correction: Head movements of subjects are a major concern in fMRI research. These movements produce local contrast changes in the MR signal and can thus result in activation artefacts. It is impossible to prevent awake human subjects from moving, at least head motion due to breathing will always occur. However, as long as the movements were not too severe, it is possible to correct them. The applied BrainVoyager 4.4 Software provides an algorithm that chooses a reference image from a data set and matches each measurement from this data set with this reference image.

c) Temporal data smoothing in the frequency domain: Slow linear drifts in the pixel time courses are not desired, as they are not likely to relate to the experimental manipulations. Therefore, de-trending was required, which was conducted by applying a temporal high-pass filter on the data set.

2) Processing of the structural data

The anatomical T1- weighted data set was acquired with a FLASH radio-pulse sequence. The resolution was 1 x 1 x 1 millimeters. For co-registration with the functional data it had to be prepared in following stages:

a) Inhomogeneity correction: The magnetic field inside the bore is not homogenous. This results in differences in signal contrast, in particular along the

anterior – posterior axis of the brain. Thus, signal contrast is higher in posterior regions of the brain, complicating adequate white-matter segmentation. White-matter segmentation is required for the reconstruction of the cortical surface. Correction for these inhomogeneities is accomplished by first manually selecting white matter voxels within and then computing a signal intensity gradient. Voxels were now corrected for this global intensity gradient, resulting in a more homogenous signal intensity distribution.

b) The anatomical data set was then transferred into the coordinate system provided by the Talairach & Tournoux stereotaxic atlas(Talairach & Tournoux, 1988).

3) Co-registration of functional and structural data

Analysing functional time-courses based on 2D slices has the disadvantage that statistical maps are computed independently for each slice regardless of the three-dimensional information. Therefore, we generated volume time courses by aligning the 2D slice-based time-courses to the structural image. Volume time courses of a scan session in the same subject were aligned to each other.

4) Pre-processing of functional volume time courses

The three-dimensional volume time courses underwent further steps of pre-processing:

a) 3D Motion Correction: Motion Correction was already applied for the two-dimensional timecourses, but this was done within the slice-planes only. To avoid head movement artefacts in the timecourses, motion correction is also required for the three-dimensional data set. To this end, one reference image is selected from the data set and all other functional images are translated and rotated in a way that they fit to the reference image. This fit is estimated by the summed squared difference of the signal intensities of the voxels.

b) Temporal data smoothing in the frequency domain: As for the two-dimensional functional timecourses, temporal smoothing was applied to the volume time courses to correct for slow trends.

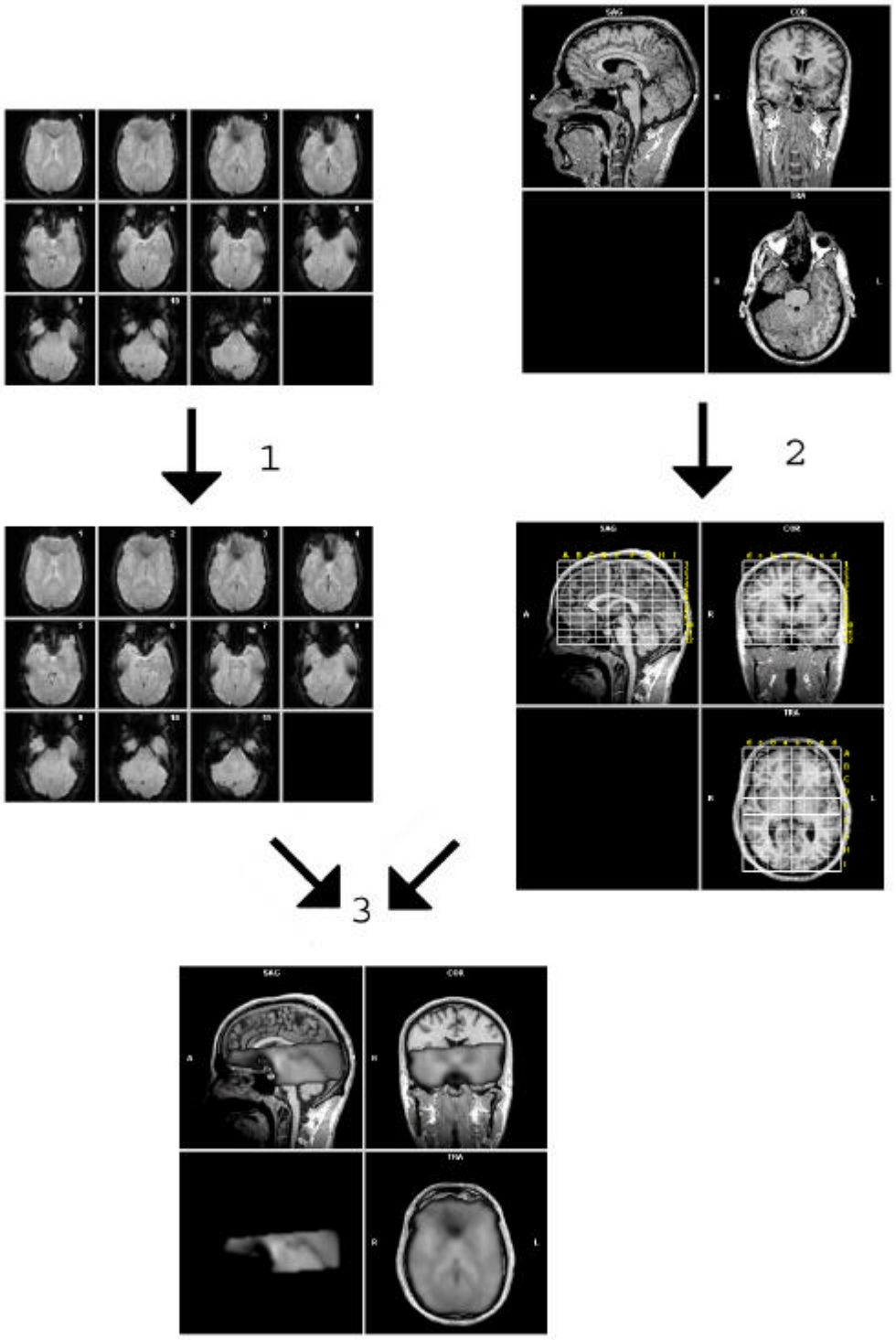

Figure C.1: This figure summarises the different stages of fMRI-data pre-processing.
1 = Pre-processing of 2D functional MRI data
(Slice scan time correction, Motion correction, Temporal smoothing)
2 = Processing of structural data
(Inhomogeneity correction, Transformation into Talairach space)
3 = Co-registration of functional and structural MRI data

Appendix D: Description of the enclosed CD -ROM

The enclosed CD-ROM contains:

1) The used stimuli saved as Tiff-picture files.

2) The behavioural data summarised in a Microsoft Office Excel file.

3) The fMRI timecourse data for each subject and the summarised data as Microsoft Office Excel files.

4) The text of this thesis as Microsoft Office Word files and as Adobe PDF file.